



Methylobacterium Genome Sequences: A Reference Blueprint to Investigate Microbial Metabolism of C1 Compounds from Natural and Industrial Sources

Citation

Vuilleumier, Stéphane, Ludmila Chistoserdova, Ming-Chun Lee, Françoise Bringel, Aurélie Lajus, Yang Zhou, Benjamin Gourion, et al. 2009. Methylobacterium genome sequences: A reference blueprint to investigate microbial metabolism of C1 compounds from natural and industrial sources. PLoS ONE 4(5): e5584.

Published Version

doi:10.1371/journal.pone.0005584

Permanent link

<http://nrs.harvard.edu/urn-3:HUL.InstRepos:4454165>

Terms of Use

This article was downloaded from Harvard University's DASH repository, and is made available under the terms and conditions applicable to Open Access Policy Articles, as set forth at <http://nrs.harvard.edu/urn-3:HUL.InstRepos:dash.current.terms-of-use#OAP>

Share Your Story

The Harvard community has made this article openly available.
Please share how this access benefits you. [Submit a story](#).

[Accessibility](#)

Methylobacterium Genome Sequences: A Reference Blueprint to Investigate Microbial Metabolism of C1 Compounds from Natural and Industrial Sources

Stéphane Vuilleumier^{1,9*}, Ludmila Chistoserdova^{2,9*}, Ming-Chun Lee³, Françoise Bringel¹, Aurélie Lajus⁴, Yang Zhou⁵, Benjamin Gourion⁶, Valérie Barbe⁷, Jean Chang⁵, Stéphane Cruveiller⁴, Carole Dossat⁷, Will Gillett⁵, Christelle Gruffaz¹, Eric Haugen⁵, Edith Hourcade¹, Ruth Levy⁵, Sophie Mangenot⁷, Emilie Muller¹, Thierry Nadalig¹, Marco Pagni⁸, Christian Penny¹, Rémi Peyraud⁶, David G. Robinson³, David Roche⁴, Zoé Rouy⁴, Channakhone Saenampekhe⁵, Grégory Salvignol⁴, David Vallenet⁴, Zaining Wu⁵, Christopher J. Marx³, Julia A. Vorholt⁶, Maynard V. Olson^{5,9,10}, Rajinder Kaul^{5,10}, Jean Weissenbach⁴, Claudine Médigue⁴, Mary E. Lidstrom^{2,11}

1 Département Micro-organismes, Génomes, Environnement, Université de Strasbourg, UMR7156 CNRS, Strasbourg, France, **2** Department of Chemical Engineering, University of Washington, Seattle, Washington, United States of America, **3** Department of Organismic and Evolutionary Biology, Harvard University, Cambridge, Massachusetts, United States of America, **4** Institut de Génomique, Laboratoire de Génomique Comparative, CEA and UMR8030 CNRS, Génomoscope, Evry, France, **5** Genome Center, University of Washington, Seattle, Washington, United States of America, **6** Institute of Microbiology, ETH Zurich, Zurich, Switzerland, **7** Institut de Génomique, CEA, Génomoscope, Evry, France, **8** Swiss Institute of Bioinformatics, Vital-IT group, Lausanne, Switzerland, **9** Department of Genome Sciences, University of Washington, Seattle, Washington, United States of America, **10** Department of Medicine, University of Washington, Seattle, Washington, United States of America, **11** Department of Microbiology, University of Washington, Seattle, Washington, United States of America

Abstract

Background: Methylotrophy describes the ability of organisms to grow on reduced organic compounds without carbon-carbon bonds. The genomes of two pink-pigmented facultative methylophilic bacteria of the Alpha-proteobacterial genus *Methylobacterium*, the reference species *Methylobacterium extorquens* strain AM1 and the dichloromethane-degrading strain DM4, were compared.

Methodology/Principal Findings: The 6.88 Mb genome of strain AM1 comprises a 5.51 Mb chromosome, a 1.26 Mb megaplasmid and three plasmids, while the 6.12 Mb genome of strain DM4 features a 5.94 Mb chromosome and two plasmids. The chromosomes are highly syntenic and share a large majority of genes, while plasmids are mostly strain-specific, with the exception of a 130 kb region of the strain AM1 megaplasmid which is syntenic to a chromosomal region of strain DM4. Both genomes contain large sets of insertion elements, many of them strain-specific, suggesting an important potential for genomic plasticity. Most of the genomic determinants associated with methylophilicity are nearly identical, with two exceptions that illustrate the metabolic and genomic versatility of *Methylobacterium*. A 126 kb dichloromethane utilization (*dcm*) gene cluster is essential for the ability of strain DM4 to use DCM as the sole carbon and energy source for growth and is unique to strain DM4. The methylamine utilization (*mau*) gene cluster is only found in strain AM1, indicating that strain DM4 employs an alternative system for growth with methylamine. The *dcm* and *mau* clusters represent two of the chromosomal genomic islands (AM1: 28; DM4: 17) that were defined. The *mau* cluster is flanked by mobile elements, but the *dcm* cluster disrupts a gene annotated as chelatase and for which we propose the name "island integration determinant" (*iid*).

Conclusion/Significance: These two genome sequences provide a platform for intra- and interspecies genomic comparisons in the genus *Methylobacterium*, and for investigations of the adaptive mechanisms which allow bacterial lineages to acquire methylophilic lifestyles.

Citation: Vuilleumier S, Chistoserdova L, Lee M-C, Bringel F, Lajus A, et al. (2009) *Methylobacterium* Genome Sequences: A Reference Blueprint to Investigate Microbial Metabolism of C1 Compounds from Natural and Industrial Sources. PLoS ONE 4(5): e5584. doi:10.1371/journal.pone.0005584

Editor: Niyaz Ahmed, University of Hyderabad, India

Received: January 24, 2009; **Accepted:** March 30, 2009; **Published:** May 18, 2009

Copyright: © 2009 Vuilleumier et al. This is an open-access article distributed under the terms of the Creative Commons Attribution License, which permits unrestricted use, distribution, and reproduction in any medium, provided the original author and source are credited.

Funding: SV was supported by a CNRS ATIP career development award, a CNRS USA mobility grant and a Génomoscope sequencing grant, and also by the Integrated Computational Genomics Resources of the Swiss Institute of Bioinformatics (RITA-CT-2006-026204) together with MP. Annotation was supported by a grant from MRT/ANR PFTV 2007, MicroScope project. CP, EH and EM were supported by PhD grants from the Government of Luxembourg, the French Ministry of Research and Région Alsace, respectively. RP was supported by ETH (ETH-25 08-2). ML, DGR, and CJM were supported by NSF (IOB-0612591), the Clarke-Cooke Fund, and the Harvard University Microbial Sciences Initiative. LC and MEL were supported by NIH (GM 58933). The funders had no role in study design, data collection and analysis, decision to publish, or preparation of the manuscript.

Competing Interests: The authors have declared that no competing interests exist.

* E-mail: vuilleumier@unistra.fr (SV); milachis@u.washington.edu (LC)

These authors contributed equally to this work.

Introduction

Pink-pigmented facultative methylotrophs of the genus *Methylobacterium* are ubiquitous in soil, air and water environments [1]. The common trait of all *Methylobacterium* species is the ability to grow on one or several reduced one carbon (C1) compounds other than methane, most prominently methanol, which is a major volatile organic compound emitted by vegetation [2]. Accordingly, strains of *Methylobacterium* are often found in association with plants, either involved in *bona fide* symbioses as endophytes, or as epiphytes on leaf surfaces [3–7]. The potential of strains from this genus to provide biotechnological products of high added value has attracted sustained scientific attention [8,9].

Of all *Methylobacterium* strains, *M. extorquens* strain AM1 (formerly *Pseudomonas* AM1, *Methylobacterium* sp. AM1) is the best studied, and has served as a model organism for over four decades. It was first isolated in 1960 in Oxford, England, as an airborne contaminant growing on methylamine [10]. It was then used as a workhorse to characterize the serine cycle for assimilation of the C1-unit of methylene tetrahydrofolate, a central intermediate in methylotrophic metabolism, and more recently the ethylmalonyl-CoA pathway for glyoxylate regeneration [8,11–13] (Fig. 1). Enzymatic systems for oxidation of both methanol [14,15] and methylamine [16], which involve the use of specific cofactors pyrroloquinoline quinone (PQQ) and tryptophan tryptophylquinone (TTQ), respectively [17], were characterized in strain AM1. Bacterial tetrahydromethanopterin (H₄MPT)-dependent enzymes, now known to occur in most methylotrophs [18,19] but originally thought to be unique to archaeal methanogens [20] were also first demonstrated in this strain. In *Methylobacterium*, the H₄MPT-dependent pathway has been shown to play a major role in both energy generation and protecting cells from formaldehyde poisoning [21]. As to the analogous tetrahydrofolate (H₄F)-linked pathway that involves two enzymes encoded by *mttA* and *fch*, also first discovered in this organism [22,23], its major role in assimilatory metabolism was recently identified in supplying C1 units into the serine cycle [24,25] (Fig. 1).

Draft genome data for *M. extorquens* AM1 have been available since 2003 [11] and have enabled transcriptomic and proteomic approaches (see e.g. [26,27]), as well as metabolomic studies (see e.g. [24,28,29]). Combined with the large complement of genetic tools developed for *Methylobacterium* (see e.g. [30,31]), this has established *M. extorquens* AM1 as a model for systems level investigations.

Methylobacterium strain DM4 has been isolated from industrial wastewater sludge in Switzerland, as part of efforts to characterize microorganisms able to degrade the organohalogenated pollutant dichloromethane (DCM) [32]. Unlike methanol and methylamine, which are mainly produced naturally, DCM is better known as a synthetic compound [33,34]. Rated as potentially carcinogenic for humans and the most highly produced chlorinated organic compound (<http://www.eurochlor.org/solvents>), DCM is highly volatile (b.p. 38°C) and water-soluble, making it a widespread contaminant in the environment [35]. Aerobic methylotrophic bacteria capable of using DCM as the sole source of carbon and energy [36] express high levels of DCM dehalogenase, which transforms DCM into formaldehyde and two molecules of HCl [37]. The genotoxic effects of DCM in both mammals [38] and bacteria [39] are due to a short-lived intermediate in the enzymatic transformation of DCM to formaldehyde [40]. Growth with DCM, as the main trait that distinguishes strain DM4 from *M. extorquens* AM1, has led to its classification as a separate *Methylobacterium* species [41]. Basing on 16S rRNA gene sequence and DNA-DNA relatedness, it was recently proposed that strain DM4 should be reclassified as *M. extorquens* [42].

The primary objective of this work was to define a fully assembled and annotated reference genomic blueprint for *Methylobacterium*, to assist future experimental investigations of methylotrophic metabolism by global approaches. We report here complete genomic sequences of strains AM1 and DM4, and describe the genomic make-up and potential for genomic plasticity that underlies the extensive capacity of *Methylobacterium* for physiological adaptation to methylotrophic lifestyles. Availability of complete genomic sequences of the two strains also provides the opportunity to define the conserved complements of genes associated with methylotrophy, and to investigate the differences between the two strains associated with strain-specific adaptations.

Results and Discussion

Genomic structure

The genome of *M. extorquens* AM1 totals 6.88 Mb and consists of five replicons: a chromosome of 5.51 Mbp (Acc. No. CP001510), a megaplasmid of 1.26 Mbp (CP001511), and three plasmids (25 kb (CP001512), 38 kb (CP001513), and 44 kb (CP001514)), with an average GC content of 68.5% (Table 1, Fig. 2). The genome of strain DM4 is somewhat smaller (6.12 Mb), and features only three replicons: a chromosome of 5.94 Mbp (Acc. No. FP103042) and two plasmids (141 kb (FP103043) and 38 kb (FP103044)), with an average GC content of 68.0% (Table 1, Fig. 2). Based on their sizes and the relative distribution of sequencing reads for each replicon, plasmids p1META and p2META are predicted to be present at 2–3 copies per strain AM1 genome, the replicon p3META at 1–2 copies per genome, and the megaplasmid at one copy per genome. Predicted copy numbers of 0.4–0.5 and 0.6–0.7 per genome were obtained for DM4 plasmids p1METDI and p2METDI, respectively.

By convention, the origin of both chromosomes was set upstream of the *dnaA* gene, as no GC skew was observed to help in predict initiation and termination of replication [43]. The chromosomes of the two strains are remarkably similar in both gene content and synteny (Fig. 2, Fig. 3). 85% of the *M. extorquens* AM1 chromosomal genes have full-length homologs (higher than 30% identity) on the chromosome of strain DM4. Of these, 89% have homologs at higher than 95% identity, underlining the orthologous nature of most genes in the two strains. Ribosomal genes (23S, 16S, and 5S) are identical in all five copies of the ribosomal operon of strains AM1 and DM4. The intergenic spacer length between 16S and 23S genes is identical in all five copies of the ribosomal operon of the same strain, but its length differs markedly between the two strains (905 nt in *M. extorquens* AM1, 602 nt in strain DM4). These data confirm the already mentioned recent suggestion [42] that strain DM4 belongs to the species *M. extorquens*.

The distribution of functional categories according to the COG classification ([44], Table 2) was as expected for a free-living proteobacterium with a versatile lifestyle and the observed genome size. COG functional class assignments are more frequent and diverse for chromosomal genes than for plasmid genes (Table 2). No significant differences in functional classes were evident between AM1 and DM4 chromosomes, except for the larger proportion of genes associated with recombination, replication and repair in strain AM1, a reflection of the larger set of IS elements in that strain (Table 1, and see below).

The Mage annotation platform [45] and Alien Hunter [46] were used to detect genes and genome regions found in one strain but not in the other. Several unique chromosomal regions, termed genomic islands and ranging from a few genes to hundreds of

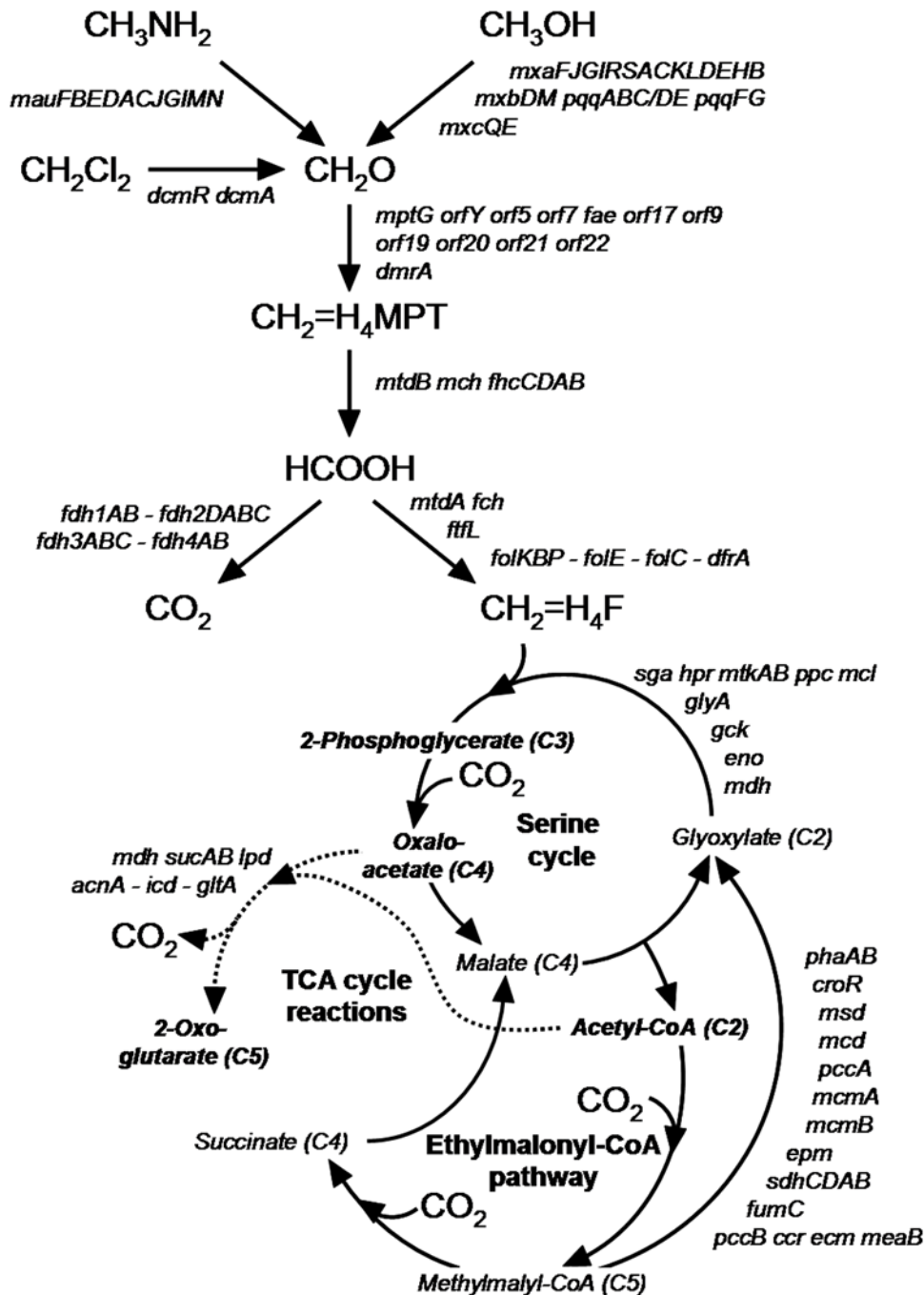


Figure 1. Central pathways for carbon conversion in *Methylobacterium* during methylo-trophic growth. Full lines, H₄MPT-dependent pathway, H₄F-dependent pathway, serine cycle and ethylmalonyl-CoA pathway for glyoxylate regeneration; broken line, tricarboxylic acid cycle reactions (2-oxoglutarate dehydrogenase activity (and a dissimilatory TCA cycle) are not essential for methylo-trophic growth [93,94]). Key pathway outputs [13] used for carbon assimilation (biomass production) are shown in bold italics. Genes involved in the serine cycle, the TCA cycle and in the ethylmalonyl-CoA pathway are indicated. Genes given on the same line and not separated by hyphens are closely associated on the chromosome. Genes and their arrangement on the chromosome are strongly conserved in strains AM1 and DM4 (see Suppl. Table S1), except the *mau* cluster for methylamine utilization and the *dcm* cluster for dichloromethane utilization which are unique to strain AM1 and strain DM4, respectively. doi:10.1371/journal.pone.0005584.g001

genes, which represent approximately 632 kb (11.5%) and 1,054 kb (17.7%) of the chromosome for strains AM1 and DM4, respectively, were defined (Table 3). With the exception of the *dcm* and *mau* gene clusters (see below), few of these islands appear to encode functions important for central metabolism or methylo-trophy. One remarkable genomic island in strain AM1 (Table 3) contains a hypothetical gene of unknown function of 47.5 kb

(META1_2412) which encodes a 15,831 residue-long repeat-rich polypeptide (Pfam PF00353 (hemolysin-type calcium-binding region); PF05594, (haemagglutinin, bacterial); COG3210 (large exoproteins involved in heme utilization or adhesion), and COG2931 (RTX toxins and related Ca²⁺-binding proteins). This gene product, if expressed, would represent one of the largest proteins known in biology [47].

Table 1. Genome statistics for *M. extorquens* AM1 and DM4.

| | Strain AM1 | Strain AM1 | Strain AM1 | Strain AM1 | Strain AM1 | Strain AM1 | Strain DM4 | Strain DM4 | Strain DM4 | Strain DM4 |
|---------------------------------|------------|-------------|-----------------|-----------------|-----------------|--------------------------|------------|-----------------|-----------------|--------------------------|
| | Chromosome | Megaplasmid | Plasmid p1META1 | Plasmid p2META1 | Plasmid p3META1 | Total/average | Chromosome | Plasmid p1METDI | Plasmid p2METDI | Total/Average |
| Size (bp) | 5511322 | 1261460 | 44195 | 37858 | 24943 | 6879778 | 5943768 | 141504 | 38579 | 6123851 |
| GC (%) | 68.7 | 67.7 | 67.9 | 65.3 | 66.9 | 68.5^a | 68.1 | 65.3 | 63.7 | 68.0^a |
| Repeat regions ^b (%) | 8.3 | 7.9 | 0.2 | 2.7 | 0.3 | 8.0^a | 9.3 | 1.6 | 0 | 9.1^a |
| Genes | 5315 | 1318 | 46 | 45 | 35 | 6759 | 5857 | 137 | 41 | 6035 |
| Protein-coding genes | 5227 | 1312 | 46 | 45 | 35 | 6665 | 5769 | 137 | 41 | 5947 |
| <i>Average length</i> | | | | | | | | | | |
| CDS (bp) | 905.3 | 846.9 | 822.7 | 693.2 | 536.6 | 891.7^a | 888.2 | 878.4 | 821.9 | 887.2^a |
| Intergenic (bp) | 178.1 | 167.7 | 163.1 | 229.2 | 160.6 | 176.4^a | 180.4 | 309.6 | 202.6 | 183.4^a |
| Coding density (%) | 84.2 | 84.1 | 78.9 | 73.1 | 69.8 | 84.0^a | 83.6 | 70.6 | 77.7 | 83.3^a |
| rRNA operons | 5 | 0 | 0 | 0 | 0 | 5 | 5 | 0 | 0 | 5 |
| tRNA | 57 | 6 | 0 | 0 | 0 | 63 | 58 | 0 | 0 | 58 |
| <i>Insertion elements (IS)</i> | | | | | | | | | | |
| Total length (%) | 2.4 | 7.6 | 22.0 | 27.5 | 15.5 | 3.7^a | 1.6 | 21.5 | 10.0 | 2.1^a |
| Intact IS ^c | 93 (19) | 41 (25) | 3 (3) | 4 (4) | 1 (1) | 142 (39) | 54 (27) | 15 (15) | 2 (2) | 71 (42) |
| Partial IS ^c | 8 (7) | 22 (13) | 1 (1) | 1 (1) | 0 | 32 (19) | 17 (11) | 5 (5) | 1 (1) | 23 (15) |
| MITEs | 1 | 3 | 0 | 0 | 0 | 4 | 8 | 0 | 0 | 8 |

^aAverage.^bDefined by the algorithm Nosferatu as implemented in Mage [45].^cNumber of IS elements (number of IS types in brackets).

doi:10.1371/journal.pone.0005584.t001

Extra-chromosomal replicons are highly strain-specific and show little similarity in size, gene content or synteny with each other. However, an approximately 130 kb region of the AM1 megaplasmid is globally syntenic to a region of similar length in the chromosome of strain DM4 (Fig. 3). Plasmids encode mostly proteins of currently unknown function (Table 2) or proteins associated with plasmid-related functions. Exceptions include a cation efflux system on plasmid p1META1 (p1META1_0021/p1META1_0022); a cluster of copper resistance genes on plasmid p2META1 (p2META1_0029/p2META1_0030); a truncated *luxI* gene (p1META1_0049) recently shown to be essential for the operation of two *bona fide*, chromosomally-located *luxI* genes, and encoding two acyl homoserine lactone synthases [48]; and UmuDC systems involved in SOS DNA repair. Unlike in strain DM4, which has two complete copies of *umuDC* on its chromosome (METDI0144/METDI0143 and METDI4328/METDI4329), a complete *umuDC* cluster in AM1 is only found on the megaplasmid (META2_0643/META2_0644), while a truncated copy of *umuC* is found on the chromosome (META1_4790).

Comparative genomics of aerobic methylotrophy

Methylotrophy can be envisioned in terms of the assembly of discrete metabolic modules, each responsible for a specific metabolic task, which in combination define pathways for methylotrophic metabolism, several variants of which have been well characterized [11,49].

The *Methylobacterium blueprint*. In *Methylobacterium*, the currently recognized methylotrophy genes and modules are found exclusively on the chromosomes of strains AM1 and DM4 (Fig. 2, Suppl. Table S1). Common genes associated with methylotrophy inventoried in Suppl. Table S1 display at least 95% identity at the protein level (99.1% average), with complete synteny between the

two strains [11]. Several methylotrophy genes are found as singletons, including several cases of genes that encode different subunits of the same enzyme (e.g. *mcmAB*, *pccAB*, see Suppl. Table S1). Nevertheless, a majority of methylotrophy genes are found in large clusters. Only two known methylotrophy gene clusters are not shared between the two strains (Suppl. Table S1, and see below): the *dcm* (dichloromethane degradation) gene region present only in strain DM4, and the *mau* gene cluster encoding methylamine dehydrogenase and accessory functions in strain AM1. One large multi-operon cluster (49.3 kb) encodes most of the serine cycle enzymes, most of the PQQ biosynthesis functions [17], genes for H₄MPT-linked reactions and H₄MPT biosynthesis, and H₄F biosynthesis genes. It also contains genes encoding a homolog of methanol dehydrogenase (XoxFJG) of still unknown function, often found nearby genes involved in C₁ metabolism [50,51] and recently suggested to be involved in formaldehyde metabolism in the photosynthetic bacterium *Rhodobacter sphaeroides* [52].

Comparison of gene sets for methylotrophy in fully sequenced genomes. A steadily increasing number of genomes of methylotrophic microorganisms have been sequenced, assembled and annotated. We limit our comparative analysis of known genetic determinants and modules of methylotrophy (Suppl. Table S2) to completed, manually annotated and officially published methylotroph genomes (listed in Suppl. Table S3), six of which belong to the phylum *Proteobacteria* and one to the phylum *Verrucomicrobia*. *Methylococcus capsulatus* represents Gamma-proteobacterial methanotrophs [53], while *Methylibium petroleiphilum* [54], *Methylobacillus flagellatus* [55] and *Methylophilales* strain HTCC2181 [56] feature two different orders within Beta-proteobacteria (*Burkholderiales* and *Methylophilales*). *Silicibacter pomeroyi*, although not reported to grow methylotrophically, is an Alpha-proteobacterium of the family

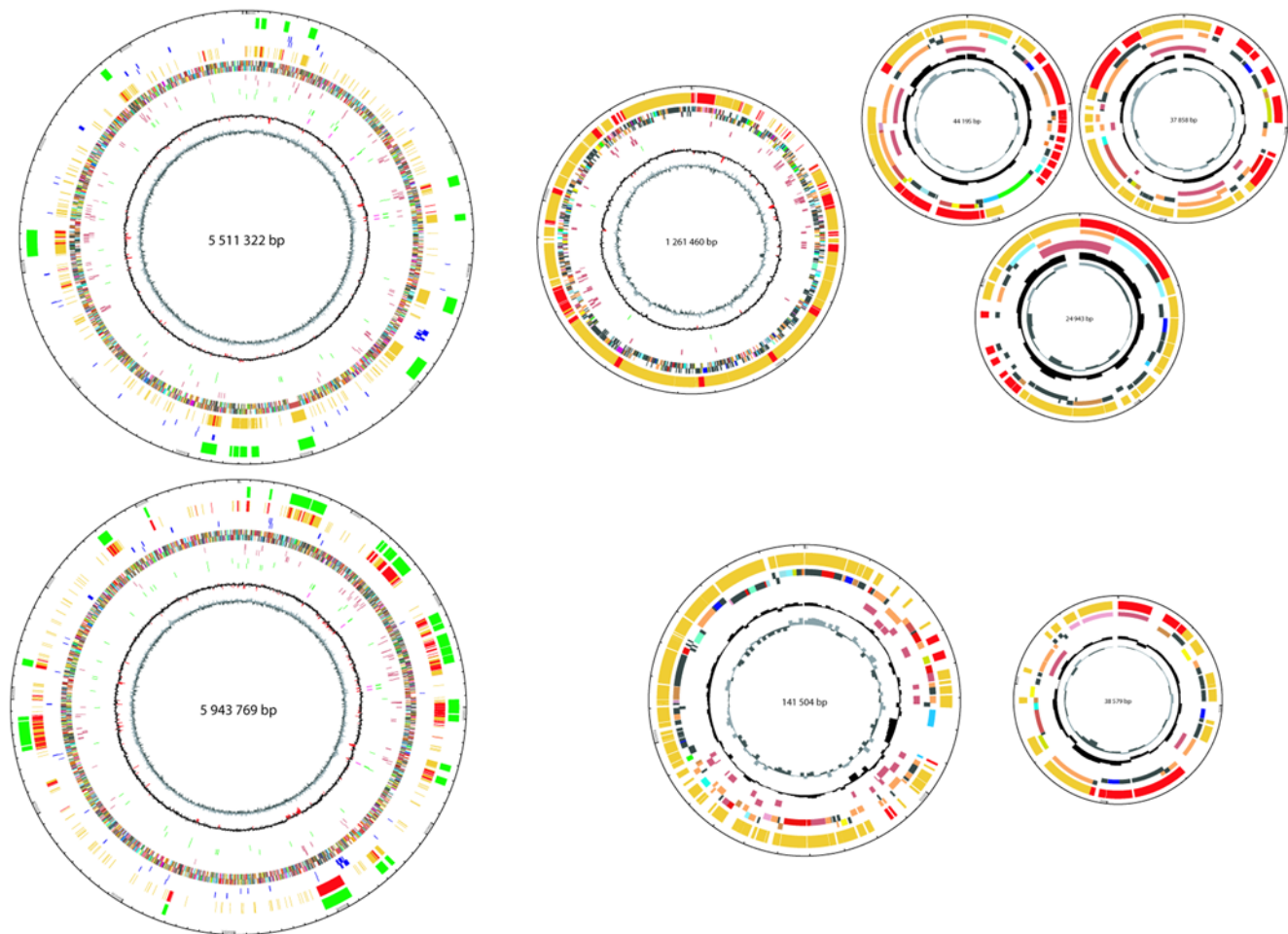


Figure 2. Schematic representation of the 8 circular replicons in the genomes of *Methylobacterium extorquens* strains AM1 (top) and DM4 (bottom). Successive circles from inside to outside: GC skew; GC deviation (with values exceeding ± 2 SD indicated in red); rRNA (pink); tRNA (green); IS elements (brown); all genes coloured according to functional class (COG); methylotrophy genes (blue, see Suppl. Table S1); strain-specific genes (yellow, except genes predicted to be of foreign origin, in red); genomic islands (green, see Table 3). Plasmids are not shown to scale. doi:10.1371/journal.pone.0005584.g002

Rhodobacteriaceae capable of degrading methylated sulfur compounds [57]. *Granulibacter bethesdensis* is an emerging human pathogen of the family of *Acetobacteriaceae* within Alpha-proteobacteria [58] reported to grow on methanol [59]. Finally, strain V4 (candidateus “*Methyloacidiphilum inferorum*”) represents the recently discovered group of thermophilic and acidophilic methanotrophs of the phylum Verrucomicrobia [60].

Methanol utilization. The *mx*a gene cluster encoding the classic methanol dehydrogenase is nearly identical (over 99% identity at the protein level) between strains AM1 and DM4, and very similar in the genomes of *M. capsulatus*, *M. flagellatus*, *G. bethesdensis* and several other proteobacterial methylotrophs [61]. This conservation of both gene sequence and gene synteny suggests that the *mx*a gene cluster has most likely disseminated via lateral transfer among methylotrophs of different subclasses of Proteobacteria. This notwithstanding, no similar gene clusters are recognizable in the genomes of the other four organisms discussed here. *M. petroleiphilum* features a gene cluster encoding an alternative methanol dehydrogenase (Mdh2; [61]) with little homology to either *mx*aF or *xox*F. The gene *xox*F is found in all of the genomes discussed here except that of *S. pomeroyi* but, as discussed elsewhere [61], the Xox system is unlikely to be responsible for aerobic methanol oxidation. The genes

responsible for methanol oxidation by *Methylophilales* HTCC2181 and strain V4 remain unknown, suggesting the existence of other, yet unidentified systems for methanol dissimilation.

Methylamine utilization. The *mau* gene cluster encoding the canonical system for methylamine utilization was characterized for a large part in strain AM1, and the genome of *M. flagellatus* [55] contains a *mau* gene cluster very similar to it. The main difference is that the gene for the electron acceptor from methylamine dehydrogenase in strain AM1, amicyanin, is replaced by a gene for azurin, an analogous copper-containing electron acceptor protein in *M. flagellatus*. The *mau* cluster was not found in genomes of the other methylotrophs including strain DM4 discussed here, which were shown or assumed to grow with methylamine (Suppl. Table S2). Thus, as yet uncharacterized genetic determinants are responsible for methylamine utilization in most methylotrophs, including strain DM4 in particular.

H₄MPT-dependent formaldehyde oxidation. Tetrahydromethanopterin (H₄MPT)-dependent formaldehyde oxidation is the main pathway for both energy generation and formaldehyde detoxification in *M. extorquens*, and therefore absolutely essential for methylotrophy in this organism [21,62,63]. First defined in *M. extorquens* AM1, this pathway has also been described in a variety of other bacteria, including from

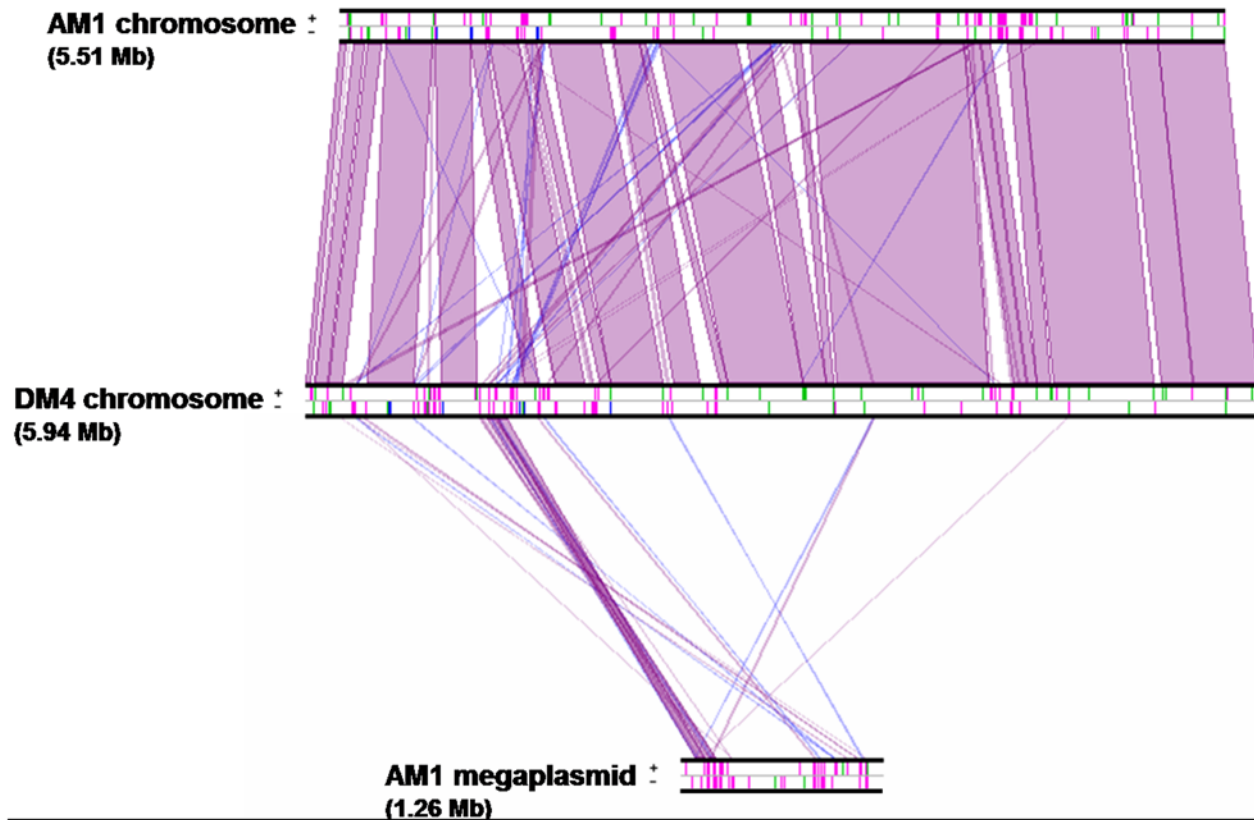


Figure 3. Overall synteny between *M. extorquens* AM1 and DM4. The linearized replicons were aligned and visualized by Lineplot in Mage. Syntenic relationships comprising at least 8 genes are indicated by violet and blue lines for genes found on the same strand or on opposite strands, respectively. IS elements (pink), ribosomal operons (blue) and tRNAs (green) are also indicated.
doi:10.1371/journal.pone.0005584.g003

phyla whose methylotrophic ability has not yet been demonstrated such as Planctomycetes [18,64,65]. Phylogenetic analysis suggests that this pathway must be one of the most ancient in the context of methylotrophic metabolism. However, it is unessential in *M. flagellatus* [66], and is absent in some other methylotrophs. *S. pomeroyi* possesses an alternative glutathione-dependent (FlhA/FghA) system for oxidation of formaldehyde similar to that of *P. denitrificans* [67] and *R. sphaeroides* [52]. No formaldehyde oxidation systems were identified in the genomes of *Methylophilales* HTCC2181 or *Verrucomicrobia* strain V4.

Conversion of formate to CO₂. *M. extorquens* strains possess four different functional formate dehydrogenases for the final step of energy generation from carbon oxidation [68]. The other methylotrophs included in our analysis also encode one or several FDH homologs (Suppl. Table S2), but only one, FHD2, is consistently detected. These observations suggest that formate oxidation, as a transformation ubiquitous to life, does not strictly qualify as a methylotrophy-specific reaction, and may thus involve analogous [69] enzymatic systems.

C1 assimilation via methylene tetrahydrofolate and the serine cycle. The serine cycle is essential for carbon assimilation in *Methylobacterium* and comprises reactions specific to methylotrophy as well as reactions involved in multicarbon metabolism (Fig. 1, see also [8,11]). Genes involved in the serine cycle can be ascribed to two categories on the basis of mutational analysis [11]: methylotrophy-specific genes (*glyA*, *sga*, *hpr*, *gck*, *ppc*, *mtkAB* and *mcl*), and genes which are essential under non methylotrophic growth conditions (*eno* and *mdh*). Recent evidence [24,25] and mutant analyses [23,70–73] suggest that genes for the

C1 transfer pathway linked to H₄F (*mtdA*, *fch* and *ffjL*) are specifically involved in assimilatory metabolism in *Methylobacterium*. Six methylotrophy-specific serine cycle genes, along with *mtdA* and *fch*, belong to gene clusters associated with methylotrophy on the chromosomes of strains AM1 and DM4 (Fig. 4), while the three remaining genes (*glyA*, *gck* and *ffjL*) are not parts of methylotrophy gene clusters and are located elsewhere on the chromosome.

As exemplified here for *M. petroleiphilum* [54], Beta-proteobacterial methylotrophs may also employ the serine cycle for C1 carbon assimilation [54,74]. As that of the Alpha-proteobacterium *S. pomeroyi*, the genome of *M. petroleiphilum* contains a single gene cluster encoding all required functions of the serine cycle (Fig. 4). In *S. pomeroyi* however, the organisation of this gene cluster is quite different from that of *Methylobacterium*, *Granulibacter bethesdensis* and *M. petroleiphilum* (Fig. 4), and contains tandem genes for two distantly related bifunctional methylene-H₄F dehydrogenase/methenyl-H₄F cyclohydrolase (FolD) enzymes instead of the isofunctional *mtdA/fch* genes found in the other genomes discussed here. Moreover, the *hpr*, *gck* and *sga* genes inferred from the genomic context display only modest sequence identity with *Methylobacterium* prototypes (Fig. 4), further suggesting that the serine cycle in *S. pomeroyi* belongs to an independent evolutionary lineage.

Extending the analysis to methylotrophic organisms able to grow with methane, the Gamma-proteobacterial methanotroph *M. capsulatus* also harbors serine cycle gene homologs in its genome, including the *mtdA/fch* pair, but few of them are clustered (Fig. 4). However, the gene for one key enzyme of the serine cycle, the methylotrophy-specific phosphoenolpyruvate carboxylase

Table 2. Functional classes in *M. extorquens* AM1 and DM4 replicons ^a.

| Class - Description | Strain AM1 | Strain AM1 | Strain AM1 | Strain AM1 | Strain AM1 | Strain AM1 | Strain AM1 | Strain AM1 | Strain DM4 | Strain DM4 | Strain DM4 | Strain DM4 | Strain DM4 |
|---|------------|-------------|------------|------------|------------|-------------|------------------------|------------|------------|------------|-------------|------------------------|------------|
| | Chrom. | megaplasmid | p1 | p2 | p3 | Class (%) | Proc. (%) ^a | chrom. | p1 | p2 | Class (%) | Proc. (%) ^a | |
| D - Cell cycle control, cell division, chromosome partitioning | 34 | 7 | 1 | 1 | 1 | 0.66 | 16.28 | 38 | 3 | 2 | 0.72 | 17.48 | |
| M - Cell wall/membrane/envelope biogenesis | 240 | 30 | 1 | | 1 | 4.08 | | 245 | 4 | | 4.18 | | |
| N - Cell motility | 126 | 16 | | | 3 | 2.18 | | 121 | 1 | | 2.05 | | |
| O - Posttranslational modification, protein turnover, chaperones | 164 | 32 | 2 | | | 2.97 | | 201 | 2 | | 3.41 | | |
| T - Signal transduction mechanisms | 266 | 34 | 1 | 1 | | 4.53 | | 304 | 1 | 1 | 5.14 | | |
| U - Intracellular trafficking, secretion, and vesicular transport | 35 | 8 | 1 | | | 0.66 | | 32 | 3 | | 0.59 | | |
| V - Defense mechanisms | 66 | 13 | 1 | | | 1.20 | | 80 | 2 | | 1.38 | | |
| B - Chromatin structure and dynamics | 3 | | | | | 0.05 | 14.12 | 4 | | | 0.07 | 13.28 | |
| J - Translation, ribosomal structure and biogenesis | 188 | 14 | 1 | | | 3.05 | | 199 | 1 | | 3.36 | | |
| K - Transcription | 205 | 46 | 2 | 2 | 2 | 3.86 | | 243 | 5 | 2 | 4.20 | | |
| L - Replication, recombination and repair | 292 | 161 | 11 | 11 | 3 | 7.17 | | 290 | 39 | 7 | 5.65 | | |
| C - Energy production and conversion | 262 | 26 | | 1 | | 4.34 | 24.50 | 303 | 3 | 2 | 5.18 | 27.39 | |
| E - Amino acid transport and metabolism | 423 | 31 | 1 | 1 | | 6.84 | | 468 | 12 | | 8.07 | | |
| F - Nucleotide transport and metabolism | 79 | 11 | | | | 1.35 | | 80 | | | 1.34 | | |
| G - Carbohydrate transport and metabolism | 141 | 9 | | | | 2.25 | | 144 | 1 | | 2.44 | | |
| H - Coenzyme transport and metabolism | 124 | 7 | 1 | | | 1.98 | | 123 | 1 | | 2.08 | | |
| I - Lipid transport and metabolism | 164 | 11 | | | | 2.63 | | 174 | 2 | 2 | 2.99 | | |
| P - Inorganic ion transport and metabolism | 200 | 35 | 3 | 1 | | 3.59 | | 220 | | 2 | 3.73 | | |
| Q - Secondary metabolites biosynthesis, transport and catabolism | 89 | 12 | | 1 | | 1.53 | | 92 | 1 | | 1.56 | | |
| R - General function prediction only | 355 | 40 | 2 | | | 5.96 | 11.24 | 388 | 1 | 2 | 6.57 | 12.12 | |
| S - Function unknown | 312 | 35 | 2 | 3 | | 5.28 | | 327 | 2 | 1 | 5.55 | | |
| CDS with at least one COG hit | 3768 | 578 | 30 | 22 | 10 | 4408 | 66.15 | 4076 | 84 | 21 | 4181 | 70.27 | |
| Total CDS | 5227 | 1311 | 46 | 45 | 35 | 6664 | | 5772 | 137 | 41 | 5950 | | |

^aOnly the first COG hit of each CDS is considered (CDS may be associated with several COGs).

^bProcesses: Cellular processes and signaling (D,M,N,O,T,U,V); information storage and processing (B,J,K,L); metabolism (C,E,F,G,H,I,P,Q); and poorly characterized (R,S). doi:10.1371/journal.pone.0005584.t002

Table 3. Unique regions in *M. extorquens* AM1 and DM4 chromosomes.

| Start CDS (META1_) | Start (nt) | End CDS (META1_) | End (nt) | Length (bp) | [Left border][Inside][Right border] ^a | IS | Features (proposed role) | Total CDS (%) | Unique CDS ^b (%) | AH CDS ^c (%) |
|--|------------|------------------|----------|-------------|--|--------------------|--|---------------|-----------------------------|-------------------------|
| <i>Methylobacterium extorquens</i> AM1 | | | | | | | | | | |
| 0035 | 37982 | 0046 | 51448 | 13467 | [none][GC][IS] | 1 | | 14 | 11 (78.6) | 0 |
| tRNA/0058 | 61782 | 0073 | 80559 | 18778 | [tRNA][int-AH][none] | 1 | | 17 | 16 (94.1) | 5 (29.4) |
| 0149 | 156863 | tRNA/0165 | 174721 | 17859 | [none][int-AH-mob][tRNA] | 0 | | 16 | 13 (81.3) | 0 |
| tRNA/0241 | 261958 | 0273 | 289656 | 27699 | [tRNA][GC][IS] | 4 (1) | | 34 | 25 (73.5) | 0 |
| 1078 | 1126013 | 1115 | 1164815 | 38802 | [IS][GC-mob-tRNA-tRNA][IS] | 8 | | 45 | 19 (42.2) | 4 (8.9) |
| 1226 | 1283284 | 1257 | 1308115 | 24832 | [none][GC][tRNA] | 0 | sulfur metabolism | 33 | 29 (87.9) | 0 |
| tRNA/1555 | 1629314 | 1614 | 1691767 | 62454 | [tRNA][none][IS] | 2 | | 59 | 53 (89.8) | 0 |
| tRNA/1825 | 1911338 | 1924 | 1995805 | 84467 | [tRNA][GC][int] | 6 (1) | copper resistance | 100 | 82 (82.0) | 0 |
| 2402 | 2475649 | 2415/tRNA | 2538027 | 62379 | [none][GC][tRNA] | 0 | giant META1_2412 gene | 13 | 13 (100) | 0 |
| 2573 | 2704934 | 2598 | 2734385 | 29452 | [none][GC][none] | 0 | sulfur metabolism | 25 | 14 (56.0) | 0 |
| 2622 | 2753794 | 2652 | 2781501 | 27708 | [none][GC][none] | 0 | metal transport | 31 | 31 (100) | 0 |
| 2657 | 2787350 | META1_2681 | 2808325 | 20976 | [none][GC][integrase] | 0 | | 22 | 22 (100) | 0 |
| 2687 | 2814961 | 2697 | 2823774 | 8814 | [none][GC][none] | 0 | | 11 | 10 (90.9) | 0 |
| 2755 | 2879429 | 2817 | 2939813 | 60385 | [IS][tRNA-AH][tRNA] | 2 ^d | included <i>mau</i> gene cluster | 63 | 50 (79.4) | 10 (15.9) |
| tRNA/3934 | 4056642 | 4086 | 4163355 | 106714 | [tRNA][AH][int] | 12 (3) | phage-related | 148 | 145 (98.0) | 25 (16.9) |
| 4747 | 4874344 | 4792/tRNA | 4901372 | 27028 | [integrase][GC][tRNA] | 5 | phage-related | 43 | 41 (95.3) | 6 (14.0) |
| <i>Methylobacterium extorquens</i> DM4 | | | | | | | | | | |
| 0036 | 37946 | 0052 | 51383 | 13438 | [Mite][int - GC][IS] | 2 ^d | | 16 | 13 (81.3) | 11 (68.8) |
| 0137 | 137916 | 0147/tRNA | 146122 | 8207 | [none][AH][tRNA] | 2 (1) | SOS repair (<i>umuCD</i>) | 8 | 0 | 4 (50.0) |
| tRNA/0225 | 232397 | 0336 | 321727 | 89331 | [tRNA][AH][none] | 4 | sensors/regulators, transport; carbon metabolism | 109 | 62 (56.9) | 27 (24.8) |
| 0345 | 328235 | 0426 | 390700 | 62466 | [none][GC][int] | 1 | Beta-lactamase-like domain repeat region | 78 | 57 (73.1) | 12 (15.4) |
| 0707 | 673123 | 0725 | 683063 | 9941 | [int][AH][none] | 1 | Beta-lactamase-like domain repeat region | 17 | 11 (64.7) | 11 (64.7) |
| 0736 | 689280 | 0748 | 702730 | 13451 | [none][AH][IS] | 2 (1) | efflux determinant | 14 | 13 (92.9) | 13 (92.9) |
| 0769 | 717385 | 0782 | 730568 | 13184 | [none][GC][none] | 0 | carbon metabolism | 13 | 10 (76.9) | 0 |
| 0786 | 733379 | 0825/tRNA | 759448 | 26070 | [none][AH][tRNA] | 1 ^d | gene decay region | 39 | 34 (87.2) | 28 (71.8) |
| tRNA/0840 | 774084 | 0935 | 848713 | 74630 | [tRNA][int-mob(3)-int-AH][none] | 8 ^d (3) | contains putative 5-formyl-H ₄ F cyclo-ligase | 93 | 37 (39.8) | 30 (32.3) |
| 1157 | 1065633 | 1204 | 1108451 | 42819 | [int][int-int-AH][none] | 2 (1) | | 45 | 25 (55.6) | 19 (42.2) |
| 1209 | 1114522 | 1243 | 1136772 | 22251 | [none][GC][none] | 0 | | 34 | 26 (76.5) | 10 (29.4) |
| 1275 | 1161654 | 1336 | 1215594 | 53941 | [none][GC][none] | 5 (3) | | 62 | 21 (33.9) | 19 (30.6) |
| 1341 | 1219900 | 1375 | 1252518 | 32619 | [none][GC-AH][none] | 1 ^d | copper resistance | 36 | 5 (13.9) | 3 (8.3) |
| 1382 | 1257095 | 1424 | 1290282 | 33188 | [none][AH][IS] | 5 | metal resistance | 41 | 35 (85.4) | 16 (39.0) |
| 1586 | 1452662 | 1650 | 1512578 | 59917 | [none][GC][none] | 7 ^d (4) | | 66 | 54 (81.8) | 45 (68.2) |
| 1656 | 1520241 | 1683 | 1548181 | 27941 | [none][GC][none] | 0 | putative sulfur compound transport/amidase region | 28 | 26 (92.9) | 9 (32.1) |
| 1860 | 1741524 | 1886 | 1767524 | 26001 | [none][GC][none] | 0 | carbon utilisation, transport, 25 molybdopterin-related | 25 | 25 (100) | 0 |
| 1917 | 1800884 | 1956 | 1830642 | 29759 | [none][GC][none] | 3 ^d | carbon utilisation, transport, 36 amide-related | 36 | 27 (75.0) | 18 (50.0) |
| tRNA/2330 | 2227106 | 2333 | 2244311 | 17206 | [tRNA][none][IS] | 1 (1) | | 4 | 4 (100) | 0 |
| 2348 | 2263918 | 2380 | 2300422 | 36505 | [none][GC-AH][none] | 0 | | 33 | 27 (81.8) | 6 (18.2) |
| 2551 | 2460335 | 2682 | 2587253 | 126919 | [none][mob-tRNA-int-AH][none] | 6 (1) | <i>dcm</i> region | 129 | 127 (98.4) | 127 (98.4) |
| tRNA/3361 | 3293492 | 3383 | 3308142 | 14651 | [tRNA][tRNA-int-AH][int] | 0 | | 23 | 19 (82.6) | 19 (82.6) |
| 4329 | 4266669 | 4356 | 4283718 | 17050 | [none][AH][int] | 3 | | 27 | 18 (66.7) | 10 (37.0) |
| 4367 | 4291118 | 4487 | 4393993 | 102876 | [none][AH][none] | 5 ^d | nitrogen metabolism, urease-like operon | 122 | 108 (88.5) | 59 (48.4) |

Table 3. Cont.

| Start CDS (META1_) | Start (nt) | End CDS (META1_) | End (nt) | Length (bp) | [Left border][Inside][Right border] ^a | IS | Features (proposed role) | Total CDS (%) | Unique CDS ^b (%) | AH CDS ^c (%) |
|--------------------|------------|------------------|----------|-------------|--|----|--------------------------|---------------|-----------------------------|-------------------------|
| 4495 | 4400484 | 4514 | 4415275 | 14792 | [IS][AH][IS] | 2 | | 20 | 16 (80.0) | 16 (80.0) |
| tRNA/4746 | 4641080 | 4776 | 4668490 | 27411 | [tRNA][int-mob-tRNA-AH][none] | 0 | efflux determinant | 30 | 26 (86.7) | 14 (46.7) |
| tRNA/5356 | 5288636 | 5390 | 5336993 | 48358 | [tRNA][int][none] | 0 | virulence determinant | 35 | 32 (91.4) | 22 (62.9) |
| tRNA/5552 | 5522860 | 5566 | 5532024 | 9165 | [tRNA][int-AH][none] | 20 | | 16 | 15 (93.8) | 15 (93.8) |

^aint: integrase; mob: mobility determinant; GC: region with atypical GC content; AH: region rich in genes detected by Alien Hunter; IS: Insertion Sequence; MITE: Miniature Inverted Repeat Transposable Element.

^bno homolog with >80% identity/0.8 minLap value in the chromosome of the compared strain.

^cas detected by Alien Hunter ([46], see Materials and Methods).

^dincluding one putative MITE.

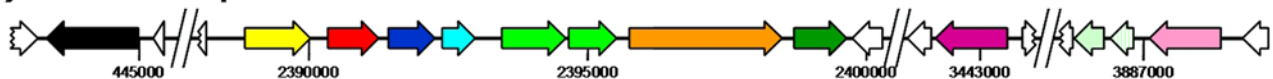
doi:10.1371/journal.pone.0005584.t003

gene, is missing [53], consistent with the extensive biochemical studies demonstrating that the main pathway for C1 assimilation in *Methylococcus capsulatus* is the RuMP pathway.

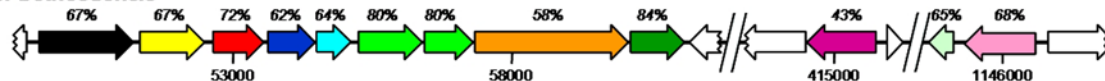
C1 assimilation and the ethylmalonyl-CoA pathway for glyoxylate regeneration. The assimilation of C1 units by the serine cycle requires the regeneration of glyoxylate from acetyl-CoA. It has been a long standing puzzle how strain AM1 achieves this given that it lacks isocitrate lyase activity, the key enzyme of the classical glyoxylate regeneration pathway [8]. Indeed, and the

corresponding gene was not detected in the *Methylobacterium* genome. Glyoxylate regeneration via the recently elucidated ethylmalonyl-CoA pathway [12] has now been demonstrated in strain AM1 [13], and the corresponding genes have been identified [11,12]. The genomes of the other bacteria compared here present a contrasting picture in this respect. The genome of *S. pomeroyi* also contains a complete set of the genes for the ethylmalonyl-CoA pathway (not shown), and as in *M. extorquens*, these genes are not clustered on the chromosome. In *M.*

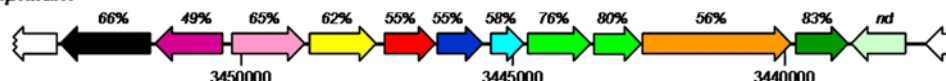
Methylobacterium extorquens AM1/DM4



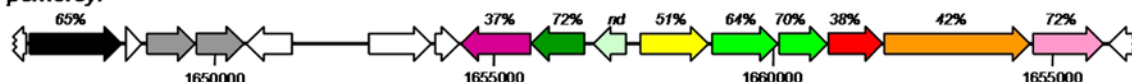
Granulibacter bethsedenis



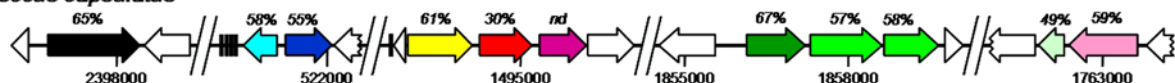
Methylibium petroleiphilum



Silicibacter pomeroyi



Methylococcus capsulatus



2 kb

Figure 4. Clustering and conservation of serine cycle and other genes important for methylotrophic metabolism in sequenced methylotrophic bacteria. Sequences were retrieved from Genbank and visualized using CLC Sequence Viewer 5 (www.clcbio.com). Chromosome sequence positions are indicated, as well as the percent identity at the protein level with *Methylobacterium* prototypes (nd: not detectable). Formate tetrahydrofolate ligase/formyl-tetrahydrofolate synthetase (*ftfl*, black); serine hydroxymethyltransferase (*glyA*, pink); serine glyoxylate aminotransferase (*sga*, yellow); hydroxypyruvate reductase (*hprA*, red); glycerate kinase (*gck*, purple); phosphoenolpyruvate carboxylase (*ppc*, orange); malyl-CoA lyase/ β -methylmalyl-CoA lyase (*mcl*, dark green); malate thiokinase (*mtkA/mtkB*, light green); NAD(P)-dependent methylene-tetrahydrofomethanopterin/methylene-tetrahydrofolate dehydrogenase (*mtdA*, dark blue); methenyl tetrahydrofolate cyclohydrolase (*fch*, light blue); bifunctional methylene-tetrahydrofolate dehydrogenase/methenyl-tetrahydrofolate cyclohydrolase (*fold*, grey); transcriptional regulator (pale green); other (white); tRNA (black rectangles).

doi:10.1371/journal.pone.0005584.g004

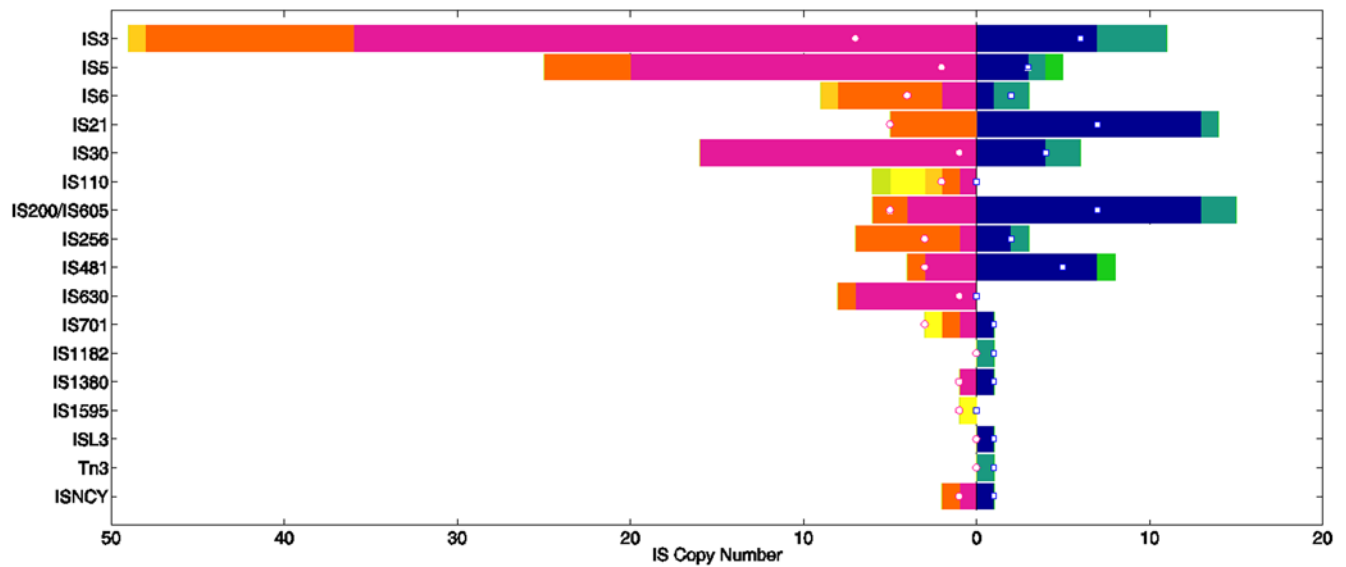


Figure 5. IS family distribution of intact ISs in *M. extorquens* AM1 and DM4. The bar length shows the total intact IS copy number of each IS family in DM4 (right) and AM1 (left) (see Suppl. Table S4). Differently colored regions represent different replicons: blue – DM4 chromosome, cyan – DM4 plasmid p1METDI, green – DM4 plasmid p2METDI, pink – AM1 chromosome, orange – AM1 megaplasmid, dark yellow – AM1 plasmid p1META1, light yellow – AM1 plasmid p2META1, light green – AM1 plasmid p3META1. Open circles and squares represent the numbers of different types of IS within each family in AM1 and DM4, respectively.
doi:10.1371/journal.pone.0005584.g005

petroleiphilum and *G. bethesdensis*, however, the genes for the key enzymes of the ethylmalonyl-CoA pathway [11] are missing (not shown), but genes thought to encode the isocitrate lyase shunt are present instead [54]. In *M. capsulatus*, neither ethylmalonyl-CoA pathway nor the isocitrate lyase shunt appear to be encoded within the genome [49], consistent with the operation of the RuMP pathway as the predominant pathway for C1 assimilation in *M. capsulatus*.

Transcriptional regulation of carbon assimilation in methylotrophic metabolism. The gene of the global serine cycle regulator in *Methylobacterium* (QscR, a LysR-type regulator homologous to CbbR), is essential for methylotrophic growth. It activates transcription of the clustered serine cycle genes as well as of *glyA*, and negatively regulates its own transcription [75] but it is not located in the proximity of known serine cycle genes in the genome. However, the genes of several probable regulators of unknown function are found nearby serine cycle genes in all methylotrophic bacteria including *Methylobacterium* discussed here (Fig. 4).

Analysis of IS elements uncovers a significant potential for genome plasticity in *Methylobacterium*

Methylobacterium genomes display an IS content comparable to that other microbial genomes [76], but with a clear differential distribution of highly diverse IS elements in AM1 and DM4 (Fig. 5, Suppl. Table S4). In AM1, 39 different IS types (defined by a 95% amino acid identity threshold), belonging to 14 IS families (defined as broad groupings of related elements in ISfinder [77]), were detected, compared to 42 IS types belonging to 14 IS families in DM4. Overall diversity of IS types is higher in DM4, but the total number of IS elements in AM1 is twice as high as in DM4 (Table 1). A total of 71 intact and 23 partial IS elements were detected in strain DM4, representing about 2% of the genome (Table 1). With 9 and 7 copies, respectively, ISMex15 and ISMex17 were the two most abundant IS elements in this strain. In comparison, strain AM1 featured 142 intact and 32 partial IS

elements, representing 3.7% of the genome (Table 1). At 37, 16 and 23 intact copies, respectively, ISMex1, ISMex2 and ISMex3 of AM1 (with average pairwise nucleotide differences between different gene copies of only 0.01%, 0.11% and 0.03% respectively), the most abundant IS elements identified, may have undergone recent expansion. In addition, one miniature inverted-repeat transposable element (MITE), MiniMdi3, was detected in both strains (Suppl. Table S4). This element (~400 bp) is related to ISMdi3 but lacks the transposase gene. Few studies so far have identified the presence of both non-autonomous and autonomous transposable elements in the same bacterial genome (see e.g. Out of a total of 70 IS types identified in this work, only 11 IS types are shared between the two strains (Suppl. Table S4, intact IS). IS5 and IS110 are the most abundant shared IS families, each family featuring 5 to 7 different types of IS (Fig. 5). This suggests that substantial IS loss and/or acquisition has occurred during the relatively short period of time since both strains have emerged from a common ancestor.

The distribution of IS element localization within each genome displays clear-cut, non-random features. Plasmids harbor a higher density of IS elements than the chromosomes. Over 20% of the length of the DM4 plasmid p2METDI and of the AM1 plasmids p1META and p2META encode IS elements. Similarly, IS elements comprise about 8% of the length of the AM1 megaplasmid (Table 1), a significantly higher proportion than in the chromosome (χ^2 test, $p < 0.0001$). Moreover, several IS families are significantly over-represented on particular replicons. For example, all 16 copies of ISMex2, an IS element belonging to the IS481 family that is specific to strain AM1, are found on its chromosome while all 5 copies of the IS elements belonging to the IS110 family are on the megaplasmid. In contrast, 13 out of the 14 copies of IS elements of this group in DM4 are located on the chromosome. For some IS elements, however, a more homogeneous distribution was noted. For example, the Tn3 family element ISMex22 unique to strain AM1 is found in one copy per replicon. Transposition immunity was described for this type of IS

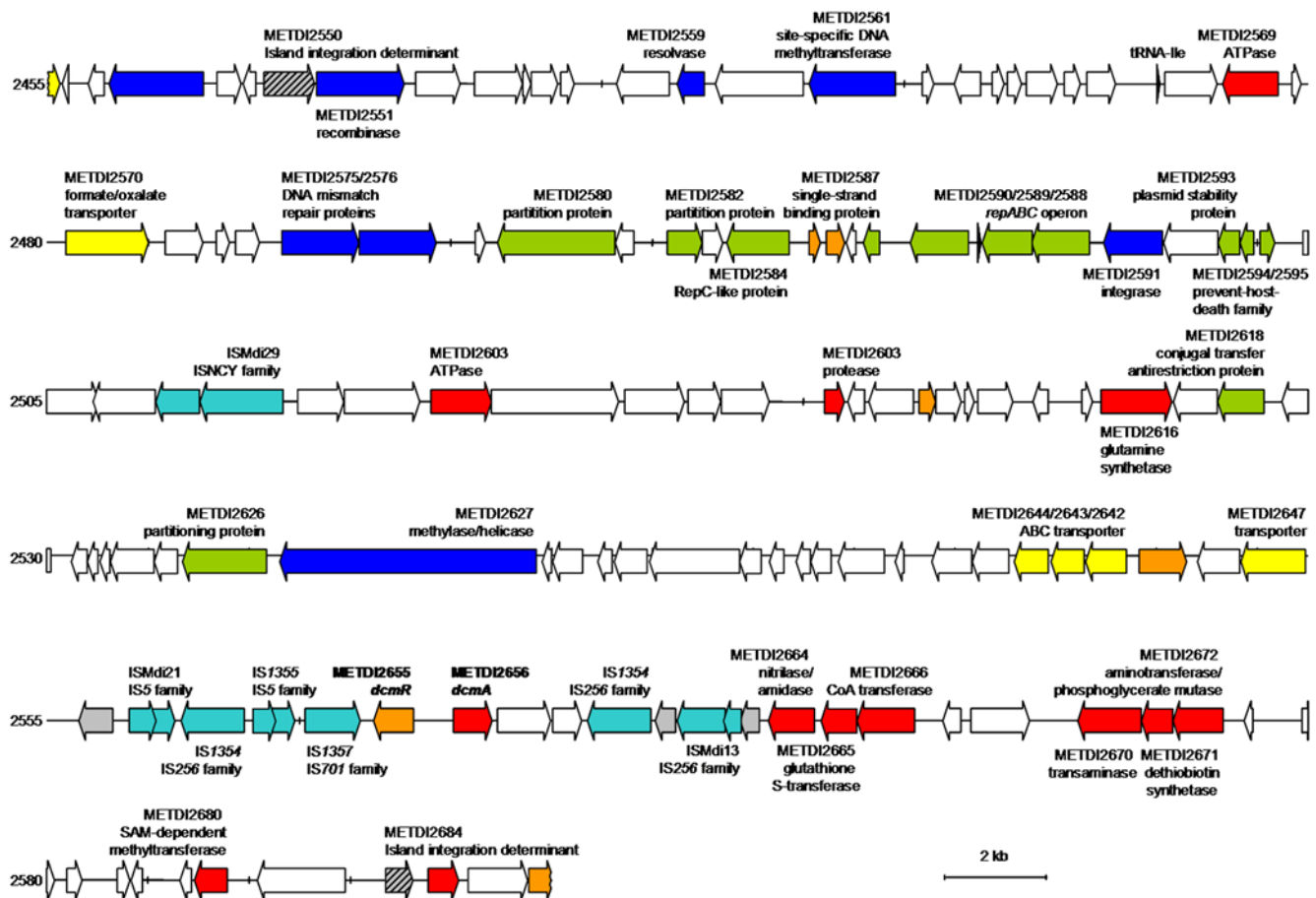


Figure 6. *dcm* region of strain DM4. All functional annotations are putative except for the DCM dehalogenase gene and its upstream regulator (bold). Highlighted are genes for putative enzymes (red), regulators (orange) transporters (yellow), proteins involved in DNA modification (blue), transposases (cyan), proteins involved in plasmid functions (green), and gene fragments (grey), with hypothetical and conserved hypothetical proteins left in white. The interrupted chelatase-like gene (hashed) defined here as “island integration determinant” flanks the 126 kb *dcm* island. doi:10.1371/journal.pone.0005584.g006

element [78], suggesting the occurrence of transposition saturation in this case.

The observed non-random IS density across replicons may be due to one or more of three potential causes: (1) biased transposition rates by different IS types across replicons, such as local hopping or plasmid specificity; (2) biased selective effects of transposition events, such as over-representation in regions with high density of genes with little or no selective value, such as plasmids or IS elements themselves; or (3) insufficient time for reaching equilibrium, e.g. for IS elements acquired via recent plasmid-mediated transmission. A second pattern in the distribution of IS locations was noted within each replicon. There is an over-representation of IS elements by 7-fold and 39-fold in chromosomal regions unique to AM1 and DM4, respectively, relative to the regions shared between the two strains (χ^2 test, $p < 0.0001$; also see Fig. 2). These could represent regions with fewer essential genes and therefore relaxed selection against DNA insertions. Alternatively, they could have been IS-rich regions dating back to the common ancestor of these two strains. This would have then led to increased rates of deletion between two co-directional copies of the same IS element, causing such IS-rich regions to be lost more frequently.

IS elements linked to methylotrophy. The two strain-specific methylotrophy regions containing *mau* (in AM1) and *dcm* (in DM4) gene clusters (Table 3) are closely associated with IS

elements. In strain DM4, genes *dcmR* and *dcmA* are embedded within several overlapping IS elements ([79], Table 3 and see below, Fig. 6). In strain AM1, the *mau* cluster (12 kb) lies between 2 copies of ISMex15 (~30 kb), as part of a larger (approx. 66 kb) gene cluster unique to this strain (Table 3). This suggests that such methylotrophy-associated gene clusters may be prone to lateral gene transfer and/or deletion. Indeed, it has been shown recently that the presence of the *mau* gene cluster is variable in closely related environmental strains of *Methylobacterium*, a betaproteobacterial methylotroph [80]. This phenomenon may be involved in the emergence of new ecotypes of methylotrophs.

The genomic island for DCM utilization: a new type of mobility determinant?

Unlike methylamine and methanol which are produced naturally in large amounts [2,81], DCM is produced naturally at low levels only [33], and presumably occurs at significant concentrations in the environment due to industrial production. The *dcm* genomic island unique to strain DM4 with the *dcmA* gene encoding DCM dehalogenase required for growth of *Methylobacterium* with DCM is located on the chromosome (Table 3, Fig. 6), just 20 genes downstream of the large conserved 49 kb methylotrophy gene cluster (Fig. 2, Suppl. Table S1). This 126 kb DNA region, of markedly different GC content (60.5%) from the genome average,

Table 4. Chelatase-like Island integration determinant (*iid*) associated with genomic islands in completed microbial genomes.

| Characteristic | <i>M. strain DM4</i> | <i>M. extorquens PA1</i> | <i>Mesorhizobium loti</i> | <i>Nitrobacter hamburgensis X14</i> |
|--|------------------------------------|---|---|--------------------------------------|
| Genome accession number | FP103042 | NC_010172 | NC_002678 | NC_007964 |
| Disrupted CDS^a | | | | |
| 5'-end fragment | METDI2550 (100) | Mext1904 (99) | MII4733 (70) | Nham144 (75) |
| Integration position | 329 | 215 | 214 | 214 |
| 3'-end fragment | METDI2684 (99) | Mext1923 (98) | MII4667 (70) | Nham130 (73) |
| Associated recombinase (Rec) | METDI2551 (+, 100) | Mext1905 (+, 28) | Mlr4668 (+, 28) | Nham143 (+, 28) |
| Genomic island organization ^c | DR-DR2-PAL-Rec-[Insert]-PAL/DR2-DR | DR/PAL-Rec-[Insert]-PAL/DR | DR/PAL1-[Insert]-Rec-PAL2/DR | DR-PAL-Rec-[Insert]-PAL/DR |
| Direct repeat (DR) sequence(s) | GAACC (DR) AA[T,A]AGA (DR2) | <u>TGCTGATGA</u> | <u>G[C,G]CACAAAT[C,G]T[G,C]CT</u> | <u>CATCA[C,T]TTGCTGA</u> |
| Palindromic (PAL) sequence(s) | ATTCCCCACCTT> X<AAGGTGGGGAAT | ATGACGTGGCCATT> X<AATAGGCCACGCAT | GCCACAATCT>GCTA< ACATTGTGGC (PAL1) GTGCAGTATTA> X<TTAATACGGCACA (PAL2) | GTGATGCTACATTA> X<TTAATGTAGCATCAC |
| Associated genomic island | | | | |
| Size (kb) | 126.4 | 18.4 | 50.5 | 17 |
| %GC ^d | 60.5 (68.1) | 69.7 (68.2) | 56.2 (62.8) | 58.2 (61.7) |
| Number of CDS | 127 | 18 | 65 | 13 |
| Proposed role | DCM degradation | Arsenite resistance | unknown | unknown |

^aCDS number, % identity at protein level and genomic island integration position relative to the intact island integration determinant CDS META1_1797 of *M. extorquens* AM1.

^bCDS number, orientation relative to the upstream island integration determinant and % identity at protein level with the recombinase of strain DM4.

^cDR: direct repeat; PAL: palindrome; Rec: recombinase. Slashes indicate sequence overlap, > and < indicate end and begin of mirror palindromic sequences. In *M. loti*, the two palindromic sequence pairs are only separated by three and four bases, respectively. Overlapping segments of direct repeat and palindromic sequences are indicated in bold or underlined (5'-end or 3'-end of the genomic island, respectively). Bases between square brackets indicate alternative bases in the corresponding motif.

^dGenome %GC content given in brackets.

doi:10.1371/journal.pone.0005584.t004

was most likely acquired by horizontal transfer. The sequences upstream and downstream of the unique *dcm* region are in complete synteny between the genomes of strains DM4 and AM1. The integration point of the *dcm* region features the 5'-end and 3'-end remains of a "chelatae-like" (COG0606, predicted ATPase with chaperone activity). Although most currently known genomic islands are located at the 3' end of a tRNA locus, other genes serving as integration sites have been described, such as the *glr* (glutamate racemase) gene of the *Helicobacter pylori* pathogenicity island [82]. Clues on the mode of integration of the *dcm* region within the *Methylobacterium* chromosomal framework were obtained by a more detailed analysis. The first CDS within the *dcm* region encodes a putative recombinase. Arrangements of non-overlapping 5' and 3' fragments of such a "chelatae" gene bordering an internal DNA fragment beginning with a recombinase gene are also evident in three other published complete genomes (Table 4). Additional DNA motifs associated with such structures include 5–20 bp direct repeats and palindromic sequences located immediately up- and downstream of the 5'- and 3'-fragments of the disrupted gene, respectively (Table 4). DNA sequences encoding "chelatae" homologs are often apparent pseudogenes, partial sequences, or sequences containing one or several internal stop codons, suggesting that such sequences may have experienced insertion and subsequent excision of DNA fragments. It is tempting to speculate that such sequences represent novel determinants of genome plasticity, and we propose the term "island integration determinant" (*iid*) to describe them.

The *dcm* region features only few genes that can be associated with confidence with methylotrophic metabolism (Fig. 6). The majority of the genes within this region (74/128, 58%) are hypothetical or conserved hypothetical proteins (compared to the chromosomal average of 41.1% and plasmid average of 43.8% for such proteins, Table 1). Several genes of the *dcm* region are interrupted by IS elements (e.g. a glutathione S-transferase METDI2660/2663), or are present in truncated form (e.g. a DNA helicase METDI2648). Many CDS seem associated with DNA modification, stability and mobility. Moreover, 7 IS elements were identified in this region, with 4 in close proximity to *dcmA* [79]. The structural elements of a *bona fide repABC* plasmid [83], i.e. a canonical *repABC* operon encoding plasmid replication and maintenance function with its counter-transcribed small RNA in divergent orientation upstream of *repC*, and a palindromic 16 nt sequence GTTCTCAGCTGAGAAC fitting the *par* binding site consensus sequence [83] upstream of *repA*, were also found within the *dcm* region. The 8 kb region centered around *repABC* displays extensive synteny with several rhizobial plasmids and with several regions on the chromosome of *Nitrobacter hamburgensis* X14 [84]. This suggests that part or all of the *dcm* region may have once existed as an extrachromosomal element and contributed to the spread of the metabolic capacity to degrade DCM in the environment. Nevertheless, introduction of the *dcmA* gene into strain AM1, with expression of active DCM dehalogenase at high levels, failed to enable growth on DCM [85]. Thus, specific adaptations are required beyond the presence of DCM dehalo-

genase to enable *Methylobacterium* to grow with this compound [36]. Additional genetic determinants needed for growth with DCM remain to be discovered, and the availability of genomic sequences will facilitate experimental efforts towards identifying them.

Conclusions

The assembled and complete genome sequences of two strains representing the pink-pigmented facultative methylotrophs of the genus *Methylobacterium* reveal extensive genome-wide homology and gene synteny. Genomic determinants of methylotrophy are almost identical between the two strains, with the exception of the methylamine utilization cluster unique to strain AM1 and of the DCM utilization cluster unique to strain DM4. Still, the two strains differ in genome size and number of replicons, and feature a set of strain-specific genes, mostly of unknown function. The large number and extensive diversity of IS elements in *Methylobacterium* genomes, along with the often clustered organization of genes for utilization of C1 compounds, suggests that genome rearrangements and horizontal gene transfer most often associated with IS elements, represent key mechanisms of *Methylobacterium* evolution relating to growth-supporting nutrients and environmental conditions. The co-linearity of the two genomes and the absence of substantial large-scale sequence rearrangements are all the more striking in this context, and may indicate that purifying selection sets strong constraints against major alterations of the genome structure in *Methylobacterium*, despite the long laboratory history of the two strains, usually grown with different carbon sources (methanol for strain AM1 and DCM for strain DM4). These two genome sequences thus afford a refined picture of the potential of *Methylobacterium* for physiological flexibility and adaptation to specific environmental constraints within a conserved genomic framework, and provide the basis for renewed, systems level experimental investigations.

Materials and Methods

Sequencing, assembly, and validation of the genome of *M. extorquens* AM1

Sequence data were obtained by whole genome shotgun sequencing as previously described [86]. BigDye terminator chemistry and capillary DNA sequencers (model 3700, Applied Biosystems) were used. Randomly picked blunt end-cloned small insert pUC19 vector-based plasmids (average ~3 kb insert size) were sequenced at both ends using universal forward and reverse sequencing primers, according to standard protocols established at the University of Washington Genome Center. In addition, a large insert fosmid library was constructed from *Sau3A* partial-restricted genomic DNA cloned in *Bam*H1 digested pFOS1 vector. About 1,920 randomly picked fosmid clones were end-sequenced and the data pooled with the small insert shotgun sequence data. Sequence data were assembled and visualized using Phred/Phrap/Consed software (www.phrap.com). The sequence quality and assembly was improved by carrying out several rounds of experiments designed by the Autofinish tool in Consed [87]. Manual finishing was carried out that involved (a) use of specialized sequencing chemistries to sequence difficult regions; (b) PCR amplification and sequencing of specific targeted regions; (c) transposon mutagenesis of over 110 small insert clones followed by sequencing to fix misassembled or difficult to assemble regions; and (d) shotgun sequencing of the 58 targeted fosmid clones to fix long-range misassemblies in the assembled genome. The consensus sequences from transposon mutagenized small insert clones, and the shotgun sequenced fosmid clones were used as backbones in the main genome assembly to resolve misassembled regions. The

final strain AM1 genome assembly contained a total of 132942 sequence reads, as well as the backbones from 58 fosmids and over 110 transposon mutagenized small insert clones, and was validated by two independent methods. The gross-scale long-range validity of the genome assembly was established by pulse-field-gel-electrophoresis, with complete agreement between the virtual and experimentally determined fingerprint patterns of the final assembled genome, either by single restriction enzyme digestion with *Pme*I or *Swa*I or by double digestion with a mixture of *Pme*I and *Swa*I restriction enzymes (data not shown). For kb scale validation of the genome assembly, fingerprint data were generated from 1673 of the paired-end-sequenced fosmid clones by digesting with three independent restriction enzymes, *Fsp*I, *Nco*I and *Sph*I. The fosmid paired-end-sequence and experimentally derived fingerprint data were used for assembly validation by comparison with the virtual fingerprint patterns from the assembled genome using the SeqTile software tools developed for this purpose at UWGC [86]. The fosmid paired-end-reads anchored the clone to a unique position in the genome, while the fingerprint data were used to compare experimentally derived fingerprints with the sequence derived virtual patterns. A complete correspondence between the virtual and experimentally derived fingerprint pattern of the genome in the three restriction enzyme domains of *Fsp*I, *Nco*I and *Sph*I was observed, thus validating the genome assembly.

Genome sequencing, assembly and validation of the genome of strain DM4

The complete sequence of the genome of strain DM4 was obtained using three different libraries. Genomic DNA was fragmented by mechanical shearing, and 3 kb (A) and 10 kb (B) inserts were cloned, respectively, into plasmid vectors pNAV (a pcDNA2.1 (Invitrogen) derivative) and pCNS (a pSU18 derivative). In addition, a large insert BAC library (25 kb inserts, C) was constructed from *Sau3A* partially digested total DNA by cloning into pBeloBAC11. Plasmid DNAs were purified and end-sequenced (79200 (A), 27648 (B), 13056 (C) paired match end-reads, respectively) using dye-terminator chemistry on ABI3730 sequencers. Assembly was realized as described [88] with Phred/Phrap/Consed software package (www.phrap.com). An additional 2170 sequences from selected clones were used in the finishing phase of assembly.

Genome annotation and bioinformatic analysis

Coding sequences were predicted using the AMIGene (Annotation of Microbial Genomes) software [89] and then submitted to automatic functional annotation using the set of tools listed in [45]. Putative orthology relationships between the two genomes were defined by gene pairs satisfying either the Bidirectional Best Hit criterion [90] or an alignment threshold (at least 40% sequence identity over at least 80% of the length of the smallest protein). These relationships were subsequently used to search for conserved gene clusters (synteny groups) among several bacterial genomes using an algorithm based on an exact graph-theoretical approach [91]. This method allowed for multiple correspondences between genes, detection of paralogy relationships, gene fusions, and chromosomal rearrangements (inversion, insertion/deletion). The 'gap' parameter, representing the maximum number of consecutive genes that are not involved in a synteny group, was set to five.

Manual validation of automatic annotations was performed in a relational database (MethylobacScope, <https://www.genoscope.cns.fr/agc/mage/wwwpkgdb/Login/log.php?pid=26>) using the MaGe web interface [45], which allows graphic visualization of

the annotations enhanced by a synchronized representation of synteny groups in other genomes chosen for comparison. Genomes were checked for the presence of genes without homologs in the parent genome using thresholds of 80% sequence identity threshold at the protein level and 80% of the length of the shorter homolog (minLrap 0.8). Chromosomal genes of potentially foreign origin were detected using Alien Hunter [46]. Potential genomic islands were searched for with the RGP (Region of Genomic Plasticity) tool of the Mage web-based interface [45] based on synteny breaks between compared genomes, and then checked the predicted regions manually. Only regions larger than 8 kb are reported here.

IS annotations were done by in-house computational tools (Robinson, Lee, Marx, unpublished) that incorporated IScan [92], followed by manual validation based on ISfinder [77]. IS elements were given names of type “ISMex3”, with “Mex” (for *M. extorquens*) and “Mdi” (for *Methylobacterium* degrading dichloromethane) indicating strains AM1 or DM4, respectively. The same type name was used for both strains for IS elements with >95% identity in protein sequence. An intact copy was defined as a sequence whose length was at least 99% of the length of the longest copy detected, and a partial IS was defined as a >500 bp fragment with >80% DNA identity to an intact copy.

Supporting Information

Table S1 Methylophony genes in *M. extorquens* AM1 and DM4

Found at: doi:10.1371/journal.pone.0005584.s001 (0.07 MB DOC)

References

- Lidstrom ME (2006) Aerobic methylophytic prokaryotes. In: Dworkin M, Falkow S, Rosenberg E, Schleifer K-H, Stackebrandt E, eds (2006) The Prokaryotes, Vol 2: Ecophysiology and Biochemistry. New York: Springer-Verlag. pp 618–634.
- Galbally IE, Kirstine W (2002) The production of methanol by flowering plants and the global cycle of methanol. *J Atmos Chem* 43: 195–229.
- Jourand P, Giraud E, Bena G, Sy A, Willems A, et al. (2004) *Methylobacterium nodulans* sp. nov., for a group of aerobic, facultatively methylophytic, legume root-nodule-forming and nitrogen-fixing bacteria. *Int J Syst Evol Microbiol* 54: 2269–2273.
- Lidstrom ME, Chistoserdova L (2002) Plants in the pink: Cytokinin production by *Methylobacterium*. *J Bacteriol* 184: 1818–1818.
- Sy A, Timmers ACJ, Knief C, Vorholt JA (2005) Methylophytic metabolism is advantageous for *Methylobacterium extorquens* during colonization of *Medicago truncatula* under competitive conditions. *Appl Environ Microbiol* 71: 7245–7252.
- Van Aken B, Yoon JM, Schnoor JL (2004) Biodegradation of nitro-substituted explosives 2,4,6-trinitrotoluene, hexahydro-1,3,5-trinitro-1,3,5-triazine, an octahydro-1,3,5,7-tetranitro-1,3,5-tetrazocine by a phytosymbiotic *Methylobacterium* sp. associated with poplar tissues (*Populus deltoides* × *nigra* DN34). *Appl Environ Microbiol* 70: 508–517.
- Abanda-Nkpaw D, Musch M, Tschiersch J, Boettner M, Schwab W (2006) Molecular interaction between *Methylobacterium extorquens* and seedlings: growth promotion, methanol consumption, and localization of the methanol emission site. *J Exp Bot* 57: 4025–4032.
- Anthony C (1982) The Biochemistry of Methylophytes. London: Academic Press.
- Schrader J, Schilling M, Holtmann D, Sell D, Villela Filho M, et al. (2009) Methanol-based industrial biotechnology: current status and future perspectives of methylophytic bacteria. *Trends Biotechnol* 27: 107–115.
- Peel D, Quayle JR (1961) Microbial growth on C1 compounds. I. Isolation and characterization of *Pseudomonas* AM1. *Biochem J* 81: 465–469.
- Chistoserdova L, Chen SW, Lapidus A, Lidstrom ME (2003) Methylophony in *Methylobacterium extorquens* AM1 from a genomic point of view. *J Bacteriol* 185: 2980–2987.
- Erb TJ, Berg IA, Brecht V, Muller M, Fuchs G, et al. (2007) Synthesis of C-5-dicarboxylic acids from C-2-units involving crotonyl-CoA carboxylase/reductase: The ethylmalonyl-CoA pathway. *Proc Natl Acad Sci U S A* 104: 10631–10636.
- Peyraud R, Kiefer P, Christen P, Massou S, Portais J-C, et al. (2009) Demonstration of the ethylmalonyl-CoA pathway using ¹³C metabolomics. *Proc Natl Acad Sci USA* 106: 4846–4851.

Table S2 Methylophony enzymes and pathways deduced from complete genomic sequences of methylophytes

Found at: doi:10.1371/journal.pone.0005584.s002 (0.04 MB DOC)

Table S3 Methylophytic bacteria with published genome sequences included in comparative analyses

Found at: doi:10.1371/journal.pone.0005584.s003 (0.04 MB DOC)

Table S4 Characteristics of IS elements in *Methylobacterium extorquens*

Found at: doi:10.1371/journal.pone.0005584.s004 (0.05 MB DOC)

Acknowledgments

Elizabeth Skovran, Sandro Roselli, Romain Lang and David Lalaouna are thanked for participation in the annotation work.

Author Contributions

Analyzed the data: SV LC MCL FB AL YZ BG SC RP DR. Contributed reagents/materials/analysis tools: SC WG MP DGR DR GS DV. Wrote the paper: SV LC MCL FB BG MP RP CJM JAV CM. Designed the initial project: SV LC MVO JW MEL. Contributed to the manual expert annotation of the two strains: SV LC MCL FB BG CG EHourcade EM TN CP RP. Comparative genomic analyses: SV LC MCL FB RP DR. Designed Figure 1: SV LC RP JAV. Designed Figure 2: ZR. Designed Figure 3: GS. Designed Figure 4: SV LC. Designed Figure 5: MCL. Designed Figure 6: SV. Secured funds to support the study: SV JW CM MEL. Shotgun sequencing and assembly: YZ VB JC CD RL SM CS ZW RK. Managed informatics resources of the project: CD EHaugen MP GS DV.

- Afolabi PR, Mohammed F, Amaratunga K, Majekodunmi O, Dales SL, et al. (2001) Site-directed mutagenesis and X-ray crystallography of the PQQ-containing quinoprotein methanol dehydrogenase and its electron acceptor, cytochrome c_L. *Biochemistry* 40: 9799–9809.
- Williams PA, Coates L, Mohammed F, Gill R, Erskine PT, et al. (2005) The atomic resolution structure of methanol dehydrogenase from *Methylobacterium extorquens*. *Acta Crystallogr Sect D-Biol Crystallogr* 61: 75–79.
- Chistoserdov AY, Chistoserdova LV, McIntire WS, Lidstrom ME (1994) Genetic organization of the *mau* gene cluster in *Methylobacterium extorquens* AM1: complete nucleotide sequence and generation and characteristics of *mau* mutants. *J Bacteriol* 176: 4052–4065.
- Davidson VL (2001) Pyrroloquinoline quinone (PQQ) from methanol dehydrogenase and tryptophan tryptophylquinone (TTQ) from methylamine dehydrogenase. *Adv Protein Chem* 58: 95–140.
- Chistoserdova L, Jenkins C, Kaluzhnaya MG, Marx CJ, Lapidus A, et al. (2004) The enigmatic *Planctomycetes* may hold a key to the origins of methanogenesis and methylophony. *Mol Biol Evol* 21: 1234–1241.
- Vorholt JA, Chistoserdova L, Stolyar SM, Thauer RK, Lidstrom ME (1999) Distribution of tetrahydromethanopterin-dependent enzymes in methylophytic bacteria and phylogeny of methenyl tetrahydromethanopterin cyclohydrolases. *J Bacteriol* 181: 5750–5757.
- Chistoserdova L, Vorholt JA, Thauer RK, Lidstrom ME (1998) C-1 transfer enzymes and coenzymes linking methylophytic bacteria and methanogenic Archaea. *Science* 281: 99–102.
- Vorholt JA, Marx CJ, Lidstrom ME, Thauer RK (2000) Novel formaldehyde-activating enzyme in *Methylobacterium extorquens* AM1 required for growth on methanol. *J Bacteriol* 182: 6645–6650.
- Vorholt JA, Chistoserdova L, Lidstrom ME, Thauer RK (1998) The NADP-dependent methylene tetrahydromethanopterin dehydrogenase in *Methylobacterium extorquens* AM1. *J Bacteriol* 180: 5351–5356.
- Pomper BK, Vorholt JA, Chistoserdova L, Lidstrom ME, Thauer RK (1999) A methenyl tetrahydromethanopterin cyclohydrolase and a methenyl tetrahydrofolate cyclohydrolase in *Methylobacterium extorquens* AM1. *Eur J Biochem* 261: 475–480.
- Marx CJ, Van Dien SJ, Lidstrom ME (2005) Flux analysis uncovers key role of functional redundancy in formaldehyde metabolism. *PLoS Biol* 3: 244–253.
- Crowther GJ, Kosály G, Lidstrom ME (2008) Formate as the main branch point for methylophytic metabolism in *Methylobacterium extorquens* AM1. *J Bacteriol* 190: 5057–5062.

26. Okubo Y, Skovran E, Guo XF, Sivam D, Lidstrom ME (2007) Implementation of microarrays for *Methylobacterium extorquens* AM1. *OMICS* 11: 325–340.
27. Bosch G, Skovran E, Xia Q, Wang T, Taub F, et al. (2008) Comprehensive proteomics of *Methylobacterium extorquens* AM1 metabolism under single carbon and nonmethylotrophic conditions. *Proteomics* 8: 3494–3505.
28. Guo XF, Lidstrom ME (2008) Metabolite profiling analysis of *Methylobacterium extorquens* AM1 by comprehensive two-dimensional gas chromatography coupled with time-of-flight mass spectrometry. *Biotechnol Bioeng* 99: 929–940.
29. Kiefer P, Portais J-C, Vorholt JA (2008) Quantitative metabolome analysis using liquid chromatography-high-resolution mass spectrometry. *Anal Biochem* 382: 94–100.
30. Marx C (2008) Development of a broad-host-range *sacB*-based vector for unmarked allelic exchange. *BMC Research Notes* 1: 1.
31. Marx CJ, Lidstrom ME (2001) Development of improved versatile broad-host-range vectors for use in methylotrophs and other Gram-negative bacteria. *Microbiology* 147: 2065–2075.
32. Galli R, Leisinger T (1985) Specialized bacterial strains for the removal of dichloromethane from industrial waste. *Conservation and Recycling* 8: 91–100.
33. Khalil MAK, Moore RM, Harper DB, Lobert JM, Erickson DJ, et al. (1999) Natural emissions of chlorine-containing gases: Reactive Chlorine Emissions Inventory. *J Geophys Res-Atmos* 104: 8333–8346.
34. McCulloch A, Aucott RL, Graedel TE, Kleiman G, Midgley PM, et al. (1999) Industrial emissions of trichloroethene, tetrachloroethene, and dichloromethane: Reactive Chlorine Emissions Inventory. *J Geophys Res-Atmos* 104: 8417–8427.
35. Keith LH, Telliard WA (1979) Priority pollutants I - a perspective view. *Environ Sci Technol* 13: 416–423.
36. Vuilleumier S (2002) Coping with a halogenated one-carbon diet: aerobic dichloromethane-mineralising bacteria. In: Reineke W, Agathos S, eds (2002) *Biotechnology for the environment, Focus on Biotechnology Series*. Dordrecht: Kluwer Academic Publishers. pp 105–131.
37. Vuilleumier S, Ivoš N, Dean M, Leisinger T (2001) Sequence variation in dichloromethane dehalogenases/glutathione S-transferases. *Microbiology* 147: 611–619.
38. Starr TB, Matanoski G, Anders MW, Andersen ME (2006) Workshop overview: Reassessment of the cancer risk of dichloromethane in humans. *Toxicological Sciences* 91: 20–28.
39. Gisi D, Leisinger T, Vuilleumier S (1999) Enzyme-mediated dichloromethane toxicity and mutagenicity of bacterial and mammalian dichloromethane-active glutathione S-transferases. *Arch Toxicol* 73: 71–79.
40. Kayser MF, Vuilleumier S (2001) Dehalogenation of dichloromethane by dichloromethane dehalogenase/glutathione S-transferase leads to the formation of DNA adducts. *J Bacteriol* 183: 5209–5212.
41. Doronina NV, Trotsenko YA, Tourouva TP, Kuznetsov BB, Leisinger T (2000) *Methylophilus helveticus* sp. nov. and *Methylobacterium dichloromethanicum* sp. nov. - Novel aerobic facultatively methylotrophic bacteria utilizing dichloromethane. *Syst Appl Microbiol* 23: 210–218.
42. Kato Y, Asahara M, Arai D, Goto K, Yokota A (2005) Reclassification of *Methylobacterium chloromethanicum* and *Methylobacterium dichloromethanicum* as later subjective synonyms of *Methylobacterium extorquens* and of *Methylobacterium lusitanum* as a later subjective synonym of *Methylobacterium rhodesianum*. *J Gen Appl Microbiol* 51: 287–299.
43. Necsulca A, Lobry JR (2007) A new method for assessing the effect of replication on DNA base composition asymmetry. *Mol Biol Evol* 24: 2169–2179.
44. Tatusov RL, Fedorova ND, Jackson JD, Jacobs AR, Kiryutin B, et al. (2003) The COG database: an updated version includes eukaryotes. *BMC Bioinformatics* 4: 41.
45. Vallenet D, Labarre L, Rouy Z, Barbe V, Bocs S, et al. (2006) MaGe: a microbial genome annotation system supported by synteny results. *Nucleic Acids Res* 34: 53–65.
46. Vernikos GS, Parkhill J (2006) Interpolated variable order motifs for identification of horizontally acquired DNA: revisiting the Salmonella pathogenicity islands. *Nucleic Acids Res* 22: 2196–2203.
47. Fukuda N, Granzier LH (2005) Titin/connectin-based modulation of the Frank-Starling mechanism of the heart. *J Muscle Res Cell Motil* 26: 319–323.
48. Nieto-Peñalver CG, Cantet F, Morin D, Haras D, Vorholt JA (2006) A plasmid-borne truncated *luxI* homolog controls quorum-sensing systems and extracellular carbohydrate production in *Methylobacterium extorquens* AM1. *J Bacteriol* 188: 7321–7324.
49. Chistoserdova L, Kalyuzhnaya MG, Lidstrom ME (2005) C₁-transfer modules: from genomics to ecology. *ASM News* 71: 521–528.
50. Chistoserdova L, Lidstrom ME (1997) Molecular and mutational analysis of a DNA region separating two methylotrophy gene clusters in *Methylobacterium extorquens* AM1. *Microbiology* 143: 1729–1736.
51. Deneff VJ, Patrauchan MA, Florizone C, Park J, Tsoi TV, et al. (2005) Growth substrate- and phase-specific expression of biphenyl, benzoate, and C-1 metabolic pathways in *Burkholderia xenovorans* LB400. *J Bacteriol* 187: 7996–8005.
52. Wilson SM, Gleisten MP, Donohue TJ (2008) Identification of proteins involved in formaldehyde metabolism by *Rhodobacter sphaeroides*. *Microbiology* 154: 296–305.
53. Ward N, Larsen O, Sakwa J, Bruseth L, Khouri H, et al. (2004) Genomic insights into methanotrophy: The complete genome sequence of *Methylococcus capsulatus* (Bath). *PLoS Biol* 2: 1616–1628.
54. Kane SR, Chakicherla AY, Chain PSG, Schmidt R, Shin MW, et al. (2007) Whole-genome analysis of the methyl tert-butyl ether-degrading beta-proteobacterium *Methylobacterium petroleiphilum* PM1. *J Bacteriol* 189: 1931–1945.
55. Chistoserdova L, Lapidus A, Han C, Goodwin L, Saunders L, et al. (2007) Genome of *Methylobacillus flagellatus*, molecular basis for obligate methylotrophy, and polyphyletic origin of methylotrophy. *J Bacteriol* 189: 4020–4027.
56. Giovannoni SJ, Hayakawa DH, Tripp HJ, Stingl U, Givan SA, et al. (2008) The small genome of an abundant coastal ocean methylotroph. *Environmental Microbiol* 10: 1771–1782.
57. Moran MA, Buchan A, Gonzalez JM, Heidelberg JF, Whitman WB, et al. (2004) Genome sequence of *Silicibacter pomeroyi* reveals adaptations to the marine environment. *Nature* 432: 910–913.
58. Greenberg DE, Porcella SF, Zelazny AM, Virtaneva K, Sturdevant DE, et al. (2007) Genome sequence analysis of the emerging human pathogenic acetic acid bacterium *Granulibacter bethesdensis*. *J Bacteriol* 189: 8727–8736.
59. Greenberg DE, Porcella SF, Stock F, Wong A, Conville PS, et al. (2006) *Granulibacter bethesdensis* gen. nov., sp. nov., a distinctive pathogenic acetic acid bacterium in the family *Acetobacteraceae*. *Int J Syst Evol Microbiol* 56: 2609–2616.
60. Hou S, Makarova KS, Saw JH, Senin P, Ly BV, et al. (2008) Complete genome sequence of the extremely acidophilic methanotroph isolate V4, “*Methylacidiphilum inferorum*”, a representative of the bacterial phylum *Verrucomicrobia*. *Biol Direct* 3: 26.
61. Kalyuzhnaya MG, Hristova KR, Lidstrom ME, Chistoserdova L (2008) Characterization of a novel methanol dehydrogenase in representatives of *Burkholderiales*: Implications for environmental detection of methylotrophy and evidence for convergent evolution. *J Bacteriol* 190: 3817–3823.
62. Chistoserdova L, Vorholt J, Thauer R, Lidstrom M (1998) C1 transfer enzymes and coenzymes linking methylotrophic bacteria and methanogenic Archaea. *Science* 281: 99–102.
63. Marx CJ, Chistoserdova L, Lidstrom ME (2003) Formaldehyde-detoxifying role of the tetrahydromethanopterin-linked pathway in *Methylobacterium extorquens* AM1. *J Bacteriol* 185: 7160–7168.
64. Bauer M, Lombardot T, Teeling H, Ward NL, Amann R, et al. (2004) Archaeal-like genes for C-1-transfer enzymes in *Planctomycetes*: Phylogenetic implications of their unexpected presence in this phylum. *J Mol Evol* 59: 571–586.
65. Marx CJ, Miller JA, Chistoserdova L, Lidstrom ME (2004) Multiple formaldehyde oxidation/detoxification pathways in *Burkholderia fungorum* LB400. *J Bacteriol* 186: 2173–2178.
66. Chistoserdova L, Gomelsky L, Vorholt JA, Gomelsky M, Tsygankov YD, et al. (2000) Analysis of two formaldehyde oxidation pathways in *Methylobacillus flagellatus* KT, a ribulose monophosphate cycle methylotroph. *Microbiology* 146: 233–238.
67. Ras J, van Ophem PW, Reijnders WN, van Spanning RJ, Duine JA, et al. (1995) Isolation, sequencing, and mutagenesis of the gene encoding NAD- and glutathione-dependent formaldehyde dehydrogenase (GD-FALDH) from *Paracoccus denitrificans*, in which GD-FALDH is essential for methylotrophic growth. *J Bacteriol* 177: 247–251.
68. Chistoserdova L, Crowther GJ, Vorholt JA, Skovran E, Portais JC, et al. (2007) Identification of a fourth formate dehydrogenase in *Methylobacterium extorquens* AM1 and confirmation of the essential role of formate oxidation in methylotrophy. *J Bacteriol* 189: 9076–9081.
69. Galperin MY, Walker DR, Koonin EV (1998) Analogous enzymes: independent inventions in enzyme evolution. *Genome Res* 8: 779–790.
70. Chistoserdova LV, Lidstrom ME (1994) Genetics of the serine cycle in *Methylobacterium extorquens* AM1: identification, sequence, and mutation of three new genes involved in C1 assimilation, *offA*, *mtkA*, and *mtkB*. *J Bacteriol* 176: 7398–7404.
71. Marx CJ, O'Brien BN, Breezee J, Lidstrom ME (2003) Novel methylotrophy genes of *Methylobacterium extorquens* AM1 identified by using transposon mutagenesis including a putative dihydromethanopterin reductase. *J Bacteriol* 185: 669–673.
72. Marx CJ, Lidstrom ME (2004) Development of an insertional expression vector system for *Methylobacterium extorquens* AM1 and generation of null mutants lacking *mtdA* and/or *feh*. *Microbiology* 150: 9–19.
73. Marx CJ, Laukel M, Vorholt JA, Lidstrom ME (2003) Purification of the formate-tetrahydrofolate ligase from *Methylobacterium extorquens* AM1 and demonstration of its requirement for methylotrophic growth. *J Bacteriol* 185: 7169–7175.
74. Kalyuzhnaya MG, De Marco P, Bowerman S, Pacheco CC, Lara JC, et al. (2006) *Methyloversatilis universalis* gen. nov., sp. nov., a novel taxon within the Betaproteobacteria represented by three methylotrophic isolates. *Int J Syst Evol Microbiol* 56: 2517–2522.
75. Kalyuzhnaya MG, Lidstrom ME (2005) QscR-mediated transcriptional activation of serine cycle genes in *Methylobacterium extorquens* AM1. *J Bacteriol* 187: 7511–7517.
76. Siguier P, Filée J, Chandler M (2006) Insertion sequences in prokaryotic genomes. *Curr Op Microbiol* 9: 526–531.
77. Siguier P, Perochon J, Lestrade L, Mahillon J, Chandler M (2006) ISfinder: the reference centre for bacterial insertion sequences. *Nucleic Acids Res* 34: D32–D36.
78. Chandler M, Mahillon J (2002) Insertion sequences revisited. In: Craig NL, Craigie R, Gellert M, Lambowitz AM, eds (2002) *Mobile DNA II*. Washington DC: ASM Press. pp 305–366.

79. Schmid-Appert M, Zoller K, Traber H, Vuilleumier S, Leisinger T (1997) Association of newly discovered IS elements with the dichloromethane utilization genes of methylophilic bacteria. *Microbiology* 143: 2557–2567.
80. Kalyuzhnaya MG, Lapidus A, Ivanova N, Copeland AC, McHardy AC, et al. (2008) High-resolution metagenomics targets specific functional types in complex microbial communities. *Nat Biotech* 26: 1029–1034.
81. Neff JC, Holland EA, Dentener FJ, McDowell WH, K.M. R (2002) The origin, composition and rates of organic nitrogen deposition: a missing piece of the nitrogen cycle? *Biogeochemistry* 57/58: 99–136.
82. Censini S, Lange C, Xiang ZY, Crabtree JE, Ghiara P, et al. (1996) *cag*, a pathogenicity island of *Helicobacter pylori*, encodes type I-specific and disease-associated virulence factors. *Proc Natl Acad Sci USA* 93: 14648–14653.
83. Cevallos MA, Cervantes-Rivera R, Gutierrez-Rios RM (2008) The *repABC* plasmid family. *Plasmid* 60: 19–37.
84. Starckenburg SR, Larimer FW, Stein LY, Klotz MG, Chain PSG, et al. (2008) Complete genome sequence of *Nitrobacter hamburgensis* X14 and comparative genomic analysis of species within the genus *Nitrobacter*. *Appl Environ Microbiol* 74: 2852–2863.
85. Kayser MF, Ucurum Z, Vuilleumier S (2002) Dichloromethane metabolism and C1 utilization genes in *Methylobacterium* strains. *Microbiology* 148: 1915–1922.
86. Rohmer L, Fong C, Abmayr S, Wasnick M, Freeman TJL, et al. (2007) Comparison of *Francisella tularensis* genomes reveals evolutionary events associated with the emergence of human pathogenic strains. *Genome Biol* 8: R102.
87. Gordon D, Desmarais C, Green P (2001) Automated finishing with Autofinish. *Genome Res* 11: 614–625.
88. Vallenet D, Nordmann P, Barbe V, Poirel L, Mangenot S, et al. (2008) Comparative analysis of Acinetobacters: Three genomes for three lifestyles. *PLoS ONE* 3: e1805.
89. Bocs S, Cruveiller S, Vallenet D, Nuel G, Medigue C (2003) AMIGene: Annotation of Microbial genes. *Nucleic Acids Res* 31: 3723–3726.
90. Overbeek R, Fonstein M, D'Souza M, Pusch GD, Maltsev N (1999) The use of gene clusters to infer functional coupling. *Proc Natl Acad Sci USA* 96: 2896–2901.
91. Boyer F, Morgat A, Labarre L, Pothier J, Viari A (2005) Syntons, metabolons and interactons: an exact graph-theoretical approach for exploring neighbourhood between genomic and functional data. *Bioinformatics* 21: 4209–4215.
92. Wagner A, Lewis C, Bichsel M (2007) A survey of bacterial insertion sequences using IScan. *Nucleic Acids Res* 35: 5284–5293.
93. Taylor IJ, Anthony C (1976) A biochemical basis for obligate methylophilicity: properties of a mutant of *Pseudomonas* AM1 lacking 2-oxoglutarate dehydrogenase. *J Gen Microbiol* 93: 259–265.
94. van Dien SJ, Okubo Y, Hough MT, Korotkova N, Taitano T, et al. (2003) Reconstruction of C-3 and C-4 metabolism in *Methylobacterium extorquens* AM1 using transposon mutagenesis. *Microbiology* 149: 601–609.